Large-scale dam removal on the Elwha River, Washington, USA: Fluvial sediment load

Christopher S. Magirl [a,*], Robert C. Hilldale [b], Christopher A. Curran [c], Jeffrey J. Duda [d], Timothy D. Straub [e], Marian Domanski [e], James R. Foreman [c]

[a] U.S. Geological Survey, Arizona Water Science Center, 520 N. Park Ave, Suite 221, Tacoma, WA 85719, United States
[b] Bureau of Reclamation, Denver Federal Center, 6th Ave. and Kipling St., Denver, CO 80225, United States
[c] U.S. Geological Survey, Washington Water Science Center, 934 Broadway, Suite 300, Tacoma, WA 94802, United States
[d] U.S. Geological Survey, Western Fisheries Research Center, 6505 NE 65th St., Seattle, WA 98115, United States
[e] U.S. Geological Survey, Illinois Water Science Center, 405 N. Goodwin Avenue, Urbana, IL 61801, United States

ARTICLE INFO

ABSTRACT

The Elwha River restoration project, in Washington State, includes the largest dam-removal project in United States history to date. Starting September 2011, two nearly century-old dams that collectively contained 21 ± 3 million m^3 of sediment were removed over the course of three years with a top-down deconstruction strategy designed to meter the release of a portion of the dam-trapped sediment. Gauging with sediment-surrogate technologies during the first two years downstream from the project measured $8,200,000 \pm 3,400,000$ tonnes of transported sediment, with 1,100,000 and 7,100,000 t moving in years 1 and 2, respectively, representing 3 and 20 times the Elwha River annual sediment load of $340,000 \pm 80,000$ t/y. During the study period, the discharge in the Elwha River was greater than normal (107% in year 1 and 108% in year 2); however, the magnitudes of the peak-flow events during the study period were relatively benign with the largest discharge of 292 m^3/s (73% of the 2-year annual peak-flow event) early in the project when both extant reservoirs still retained sediment. Despite the muted peak flows, sediment transport was large, with measured suspended-sediment concentrations during the study period ranging from 44 to 16,300 mg/L and gauged bedload transport as large as 24,700 t/d. Five distinct sediment-release periods were identified when sediment loads were notably increased (when lateral erosion in the former reservoirs was active) or reduced (when reservoir retention or seasonal low flows and cessation of lateral erosion reduced sediment transport). Total suspended-sediment load was 930,000 t in year 1 and 5,400,000 t in year 2. Of the total $6,300,000 \pm 3,200,000$ t of suspended-sediment load, 3,400,000 t consisted of silt and clay and 2,900,000 t was sand. Gauged bedload on the lower Elwha River in year 2 of the project was $450,000 \pm 360,000$ t. Bedload was not quantified in year 1, but qualitative observations using bedload-surrogate instruments indicated detectable bedload starting just after full removal of the downstream dam. Using comparative studies from other sediment-laden rivers, the total ungauged fraction of <2-mm bedload was estimated to be on the order of 1.5 Mt.

Published by Elsevier B.V.

1. Introduction

As of 2013, the Elwha River restoration project involved the largest dam-removal project in United States (U.S.) history in terms of dam size, sediment volume released, and complexity of the removal strategy (U.S. Department of the Interior, 1996; Duda et al., 2011; Warrick et al., 2012, in this volume). The removal progressed with the staged deconstruction of two nearly century-old dams containing 21 ± 3 million m^3 of trapped sediment (Randle et al., in this volume) and the subsequent release (i.e., the erosion and transport by river processes) of a proportion of the trapped sediment. Modeling before the project indicated one-third to one-half of the trapped sediment would mobilize within 4–7 years after the start of the project (Randle et al., 1996; Konrad,

2009; Czuba et al., 2011a). The project is restoring ecologic and geomorphic processes to the downstream river corridor, estuary, and offshore marine complex (Gelfenbaum et al., 2011) as well as restoring ecologic connectivity and benefitting the aquatic ecosystem of the entire Elwha River watershed from the marine environment in the Strait of Juan de Fuca to the alpine ecosystem in the upper watershed within Olympic National Park (Wunderlich et al., 1994; Duda et al., 2008, 2011; Crane, 2011; Johnson, 2013).

The two dams on the Elwha River were part of the larger U.S. dam infrastructure, consisting of more than 80,000 large dams exceeding 7.6 m in height (Graf, 1999; O'Connor et al., 2008; U.S. Army Corps of Engineers, 2013). Following a period of dam construction in the middle twentieth century (O'Connor et al., 2008), many U.S. dams are now approaching their functional life expectancy (Doyle et al., 2003a), and dam-removal projects are being implemented to address fish-passage, safety, or economic issues (Poff and Hart, 2002; Doyle et al., 2003a). As

* Corresponding author. Tel.: +1 520 670 6671.
E-mail address: magirl@usgs.gov (C.S. Magirl).

of 2013, American Rivers (2014) estimated that over 1100 U.S. dams had been removed. The vast majority of these dam removals were structures smaller than 10-m tall, though a few taller dams with larger reservoir capacities have been removed (American Rivers et al., 1999; O'Connor et al., 2008; Major et al., 2012; Wilcox et al., 2014). Before the Elwha River dam removals, the tallest known dam-removal project in the U.S. was the 49-m Occidental Chem Pond Dam D on Duck Creek in Tennessee (American Rivers et al., 1999), and the tallest dam removed in the western U.S. was the 38-m tall Condit Dam, on the White Salmon River, in Washington State in October 2011 (Magirl et al., 2010; Wilcox et al., 2014).

A key factor when considering or implementing dam removal involves the potential effects of trapped sediment on geomorphic and ecosystem function (Heinz Center, 2002, 2003; Poff and Hart, 2002; Whitelaw and MacMullan, 2002; Doyle et al., 2003a). A number of studies have investigated a river's geomorphic response to dam removal using morphometric techniques (e.g., Pizzuto, 2002; Wildman and MacBroom, 2005; Pearson et al., 2011; Cannatelli and Curran, 2012; Bountry et al., 2013); yet, only a handful of dam-removal projects have concomitant sediment monitoring and analysis of sediment loads and fates during and after removal (e.g., Ahearn and Dahlgren, 2005; Riggsbee et al., 2007). The study of sediment dynamics associated with the August and November 2000 removal of a low-head dam on the Manatawny River, Pennsylvania, showed little increase in sediment transport with the dam breaching but increased transport during a large runoff event following removal (Johnson et al., 2001). Sediment data collected and analyzed after the removal of two low-head dams along Wisconsin's Koshkonong and Baraboo Rivers in 2000 showed total suspended solids downstream from the project up to 10 times the background values and elevated sediment conditions for at least 10 months following dam removal (Doyle et al., 2003b). The 2006–2008 removal of 13-m tall Milltown Dam on the Clark Fork in Montana was a larger project in terms of sediment volume and complexity because of the roughly 5 million m^3 of trapped reservoir sediment containing heavy-metal contamination. A large volume of the contaminated sediment was mechanically removed, but downstream sediment monitoring before, during, and following dam breaching allowed quantification of the release of 565,000 tonnes (t) of suspended sediment over 28 months (Sando and Lambing, 2011). The October 2011 removal of Condit Dam involved blasting a drain hole in the bottom of the concrete structure that allowed a rapid (~1.5-hour) draining of the reservoir and mobilization of much of the 1.8 million m^3 of trapped sediment (Wilcox et al., 2014). The rapid reservoir drainage resulted in hyperconcentrated flow, which inhibited traditional sediment-sampling approaches; however, photographic documentation and 15 weeks of post-removal sediment monitoring allowed analysis of the timing of sediment released (Wilcox et al., 2014). Perhaps the most comprehensive study of sediment dynamics of bedload and suspended-sediment load during dam removal was conducted with the 2007 removal of the 15-m high Marmot Dam along the Sandy River, Oregon (Major et al., 2012). In the first two years following removal, about 58% of the sediment trapped behind Marmot Dam was released, and sediment measurements and gauging at several locations allowed the analysis of the spatial and temporal patterns of sediment redistribution (Major et al., 2012).

Whether measured by dam height or volume of trapped sediment, the largest dam-removal project as of 2013 was on the Elwha River. A dam-removal strategy was adopted to allow the river to erode trapped sediment during staged, multiyear drawdowns of two dam structures. Because municipal and industrial interests use the Elwha River water downstream from both dams, monitoring of turbidity during and following the dam removal project was a priority (Warrick et al., 2012). Measuring the release of sediment during and after dam removal provided an opportunity to describe the physical response of a mountain river to an unusually large sediment release.

We document the gauged fluvial sediment loads in the Elwha River from the start of dam removal on 15 September 2011 until 15 September 2013, representing the first two years of the river-restoration project ('year 1' defined as 15 September 2011 to 14 September 2012 and 'year 2' defined as 15 September 2012 to 15 September 2013). We report suspended-sediment concentration (SSC), suspended-sediment load, and bedload along with an estimated breakdown of the size class of particles in movement when possible. We also include estimates of the natural sediment load entering the project area from upstream, comparative data of turbidity upstream and downstream from the dam removals, and an estimate of a portion of bedload that could not be measured directly. Our study focuses on quantifying temporal patterns of fluvial sediment dynamics during the Elwha River dam-removal project and is combined with complementary studies (East et al., 2015; Gelfenbaum et al., in this volume; Randle et al., in this volume) to analyze and assess the complex spatial and temporal patterns of sediment movement in the first two years of the Elwha River restoration project (Warrick et al., in this volume).

2. Study area

2.1. Elwha River restoration project background

Two hydroelectric dams on the Elwha River were removed: the 32-m tall Elwha Dam completed in 1913 at river kilometer 7.9 (Rkm; river stationing convention in kilometers upstream from the river mouth at the Strait of Juan de Fuca) and 64-m tall Glines Canyon Dam completed in 1927 at Rkm 21.6 (Fig. 1). The reservoir behind the Elwha Dam, Lake Aldwell, stored 10 million m^3 of water to a depth of 24 m above the pre-dam river elevation. The reservoir behind Glines Canyon Dam, Lake Mills, stored 50 million m^3 of water to a depth of 52 m above the pre-dam river elevation.

The history of the two Elwha River dams and their social, economic, and ecological impacts are well documented (Wunderlich et al., 1994; Duda et al., 2008, 2011; Crane, 2011; Johnson, 2013). Both dams were built without fish passage, restricting once abundant Pacific salmon populations to the river reach downstream from the Elwha Dam (Brenkman et al., 2008; Pess et al., 2008) and interfering with in-river migratory movements by resident fish. In 2011, there were four federally listed fish populations occurring in the Elwha River (Ward et al., 2008; Brenkman et al., 2012). Recognizing the opportunity to recover salmon populations via ecosystem restoration while resolving legal issues surrounding dam relicensing through the Federal Energy Regulatory Commission (Gowan et al., 2006; Winter and Crain, 2008), the U.S. Congress passed Public Law 102-495 in 1992, paving the way for river restoration and dam removal (U.S. Department of the Interior et al., 1994; U.S. Department of the Interior, 1995, 1996).

To mitigate downstream effects from released sediment, a staged drawdown strategy was adopted governing the pace of removal and allowing sediment erosion by river processes (Randle et al., 1996). Using a series of progressive drawdown notches, the structure of each dam was lowered incrementally to allow first a redistribution of accumulated sediment into shrinking reservoirs and then a metered release of sediment to downstream reaches. Hold periods were built into the removal schedule to mitigate sediment impacts on migrating fishes. The total anticipated time of removal for both dams was 2–3 years. The Elwha Dam was fully removed by May 2012 in the first 9 months of the project (Randle et al., in this volume). As of September 2013, all but 15.3 m of Glines Canyon Dam had been removed.

2.2. Elwha River hydrology and geomorphology

The Elwha River originates in the glaciated Olympic Mountain Range, located on the Olympic Peninsula of Washington State. From its headwaters rising to over 2200 m, the river flows northward for 72 km draining an 834-km^2 catchment through a series of bounded alluvial valleys separated by bedrock canyons (Kloehn et al., 2008; Warrick et al., 2011) before
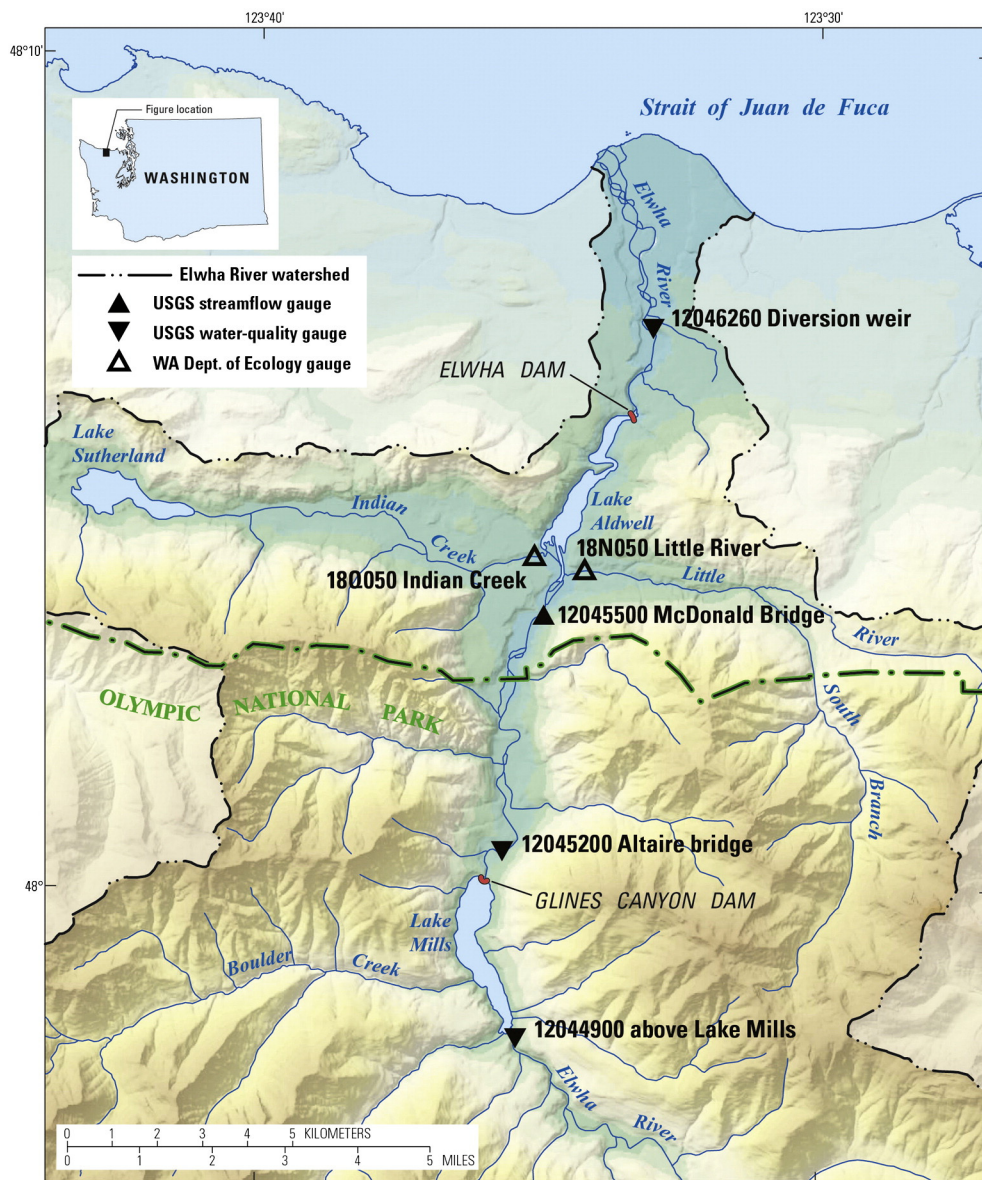
Fig. 1. Map showing the lower portion of the Elwha River watershed with inset showing where the watershed occurs in Washington State, USA. The Elwha River is shown prior to the removal of the Elwha Dam, impounding Lake Aldwell, and Glines Canyon Dam, impounding Lake Mills.

reaching the marine environment at the Strait of Juan de Fuca (Fig. 1). A maritime climate produces mild summers and cool, wet winters; precipitation falls mostly as rain in lower elevations (<1200 m) and as snow at higher elevations. Because of the rain shadow of the Olympic Mountain Range, a steep precipitation gradient exists in the watershed, with 6000 mm and 1000 mm precipitation falling near the headwaters and river mouth, respectively (average 1430 mm; Duda et al., 2011).

The hydrology of the Elwha River is characterized by two peak-flow seasons: the first during the early winter (November to January) and the second during the spring snowmelt (May to June). The largest floods are associated with heavy, sustained rainfall caused by atmospheric rivers, synoptic weather systems that tap into ample sources of tropical atmospheric water vapor (Neiman et al., 2011). Long-term records indicate that 78% of annual peak flows occur between November and January. The U.S. Geological Survey (USGS) has measured discharge in the Elwha River at McDonald Bridge (USGS streamflow-gauging station #12045500; Fig. 1) continuously since 1918: the mean annual discharge is 42.8 m^3/s. The 2-year, 10-year, and 100-year recurrence-interval floods are 400 m^3/s, 752 m^3/s, and 1240 m^3/s, respectively (Duda et al., 2011).

2.3. Long-term Elwha River sediment load

Pre-dam-removal surveys determined the volume of sediment trapped in Lake Mills in 2010 was 16 ± 2.4 million m^3, composed of approximately 46% silt and clay (<0.063 mm) and 54% sand and coarser material (Randle et al., in this volume). The Lake Mills reservoir capacity was 50 million m^3 and the total annual inflow of water from the upper Elwha River, based on data from the above Lake Mills gauge (#12044900), is 1.22 × 10^9 m^3/y, thus resulting in a capacity-to-inflow ratio (C/I) of 0.041. Using an empirical relation for reservoir trap efficiency as a function of C/I (Brune, 1953) and noting that the elongated nature of the Elwha River clasts likely increases settling velocity (Childers et al., 2000), we estimated that the trap efficiency of Lake Mills was 80 ± 10%. Bulk density of the Elwha River sediment in Lake Mills was reported to be 1.7 ± 0.2 t/m^3 for sand-sized and coarser particles and 1.1 ± 0.1 t/m^3 for silt and clay (Randle et al., in this volume). Glines Canyon Dam construction lasted from 1925 to 1927 (Randle et al., 1996). Assuming 84 years of sediment accumulation (1926 to 2010) and combining the total reservoir sediment volume with assumptions of bulk density and trap efficiency enabled us to calculate

the long-term sediment discharge from the upper Elwha River to be 340,000 ± 80,000 t/y.

3. Methods

3.1. Hydrology

Discharge was measured on 15-minute increments during the study period at the McDonald Bridge gauge, located between both dam sites (Fig. 1; Table 1), and downloaded from the National Water Information System (U.S. Geological Survey, 2014a). We estimated discharge upstream and downstream from the project area (at the above Lake Mills gauge, #12044900, and at the diversion-weir gauge, #12046260) by scaling McDonald Bridge discharge data using basin hydrology and average precipitation depths (Table 1). We further corrected upstream and downstream discharge estimates using available tributary gauging data, models to estimate ungauged tributary input, and wave routing to compensate for time of travel of flood waves between gauges. Methodological details explaining our techniques to estimate the Elwha River discharge values are given in Appendix A.

3.2. Measuring and gauging suspended-sediment concentration

Suspended-sediment sampling, combined with gauging from three sediment-surrogate instruments including two turbidimeters and an acoustic Doppler velocity meter (ADVM), allowed us to produce a near continuous record of SSC at the diversion-weir gauge during the study period. Two complementary but unique turbidimeter technologies were deployed, a nephelometer and an optical-backscatter turbidity sensor, and turbidity data were downloaded from the National Water Information System (U.S. Geological Survey, 2014a). Gaps in data collection were associated with removal of equipment for calibration or for necessary repairs following high flows (Fig. 2), but for only one day in the study period (19 November 2012) were all surrogate instruments simultaneously inoperable; on this day we used physical samples to estimate daily SSC.

We collected 24 cross section SSC samples from a pedestrian bridge 350 m downstream from the diversion-weir gauge over a range of discharge and turbidity values, and we used an automated point sampler at the gauge to collect daily composite SSC samples from September 2012 to September 2013. Limited cross-sectional, suspended-sediment samples were also collected at Altaire bridge (gauge #12045200) from October 2012 to May 2013, 1.5 km downstream from Glines Canyon Dam, to provide insight into the nature of the SSC immediately downstream from Lake Mills. Using the SSC samples, separate sediment-surrogate models were developed for each deployed surrogate technology using established techniques (Topping et al., 2004, 2006; Rasmussen et al., 2009; Wood and Teasdale, 2013). Separate sediment-surrogate models were constructed for the turbidimeters for total SSC

and for the silt and clay fraction of SSC. For all sediment-surrogate models, the calibration data consisted of discrete cross-sectional-SSC data and concurrently recorded sensor measurements. For the models developed from hydroacoustic data, the calibration data set also consisted of daily point-SSC measurements from the automated sampler, which were needed to supplement the regression data set. Point-SSC data were not used to calibrate turbidimeter-SSC models but were used as an independent data set for evaluating model performance.

Of the three operating sediment-surrogate technologies (i.e., nephelometer, optical-backscatter meter, and ADVM), no data set or analytical insight was available to indicate superior accuracy or precision of one technology over another. Therefore, after constructing the respective regression models, the SSC estimates from the operational surrogate technologies were averaged to generate the final reported daily value for SSC. Based on comparison of averaged SSC-surrogate values measured against physical samples, we assumed that the composite SSC values had an uncertainty of 50%. Notably, for low sediment conditions, particularly during the summer months, the regression models produced biased SSC values whereby SSC values appeared to be too high. This bias did not affect the accuracy of gauging heavy sediment conditions or calculating total sediment loads but did create the false impression of enhanced sediment transport at discharge values less than about 15 m³/s. Methodological details explaining our techniques to gauge SSC are given in Appendix B.

Turbidity was also measured with a nephelometer at the above Lake Mills gauge during much of the study period (Fig. 2). Because no companion suspended-sediment measurements were collected at the above Lake Mills gauge during the study, direct estimates of SSC at the above Lake Mills gauge were not made. However, paired turbidity data with common instruments allowed us to compare differences between turbidity upstream and downstream from the dam-removal project.

3.3. Calculating suspended-sediment load at diversion weir

The daily suspended-sediment load for the two-year study period was calculated at the diversion-weir gauge using the equation from Guy (1970),

$$Q_S = kQC_S\Delta t \tag{1}$$

where Q_S is suspended-sediment load in tonnes, Q is discharge at the diversion weir in m³/s, C_S is the SSC in mg/L, Δt is a time interval in days, and k is a unit-conversion coefficient equal to 0.0864. We also calculated the fractional load of silt and clay (<0.063 mm) as a subset of the total suspended-sediment load.

We assumed that the dominant source of uncertainty in calculating total suspended-sediment load was the uncertainty in SSC. When summing daily loads to calculate the total suspended-sediment load during

Table 1
Locations for gauging and hydrologic calculation along the Elwha River and its tributaries. The above Lake Mills, McDonald Bridge, and diversion-weir gauges were operated by the U.S. Geological Survey and the Indian Creek and Little River gauges were operated by the Washington State Department of Ecology. Catchment area and mean annual precipitation data from USGS (2014). n/a, not applicable; neph, nephelometric turbidity meter; OBS, optical-backscatter turbidity meter; h, stage; Q, discharge; ADVM, acoustic Doppler velocity meter; AS, automated pump samples; SSC, suspended-sediment concentration samples; BL, bedload measurements; BLIS, bedload impact sensors.

| Site	Gauge number	Elwha River kilometer	Instrumented or reported data	Operation	Catchment area, in square kilometers	Mean annual precipitation, in meters	Precipitation–volume ratio (relative to McDonald Bridge gauge)
River mouth	n/a	0	n/a	n/a	834	2.743	108.8%
Diversion-weir gauge	12046260	5.1	SSC, neph, OBS, ADVM, h, AS, BL, BLIS	2011–2013	824	2.769	108.5%
Into Lake Aldwell	n/a	11.5	n/a	n/a	807	2.794	107.3%
Little River gauge	18N050	n/a	h, Q	2011–2012	60	1.295	3.7%
Indian Creek gauge	18Q050	n/a	h, Q	n/a	49	1.580	3.7%
McDonald Bridge gauge	12045500	13.5	OBS, h, Q	2011–2013	695	3.023	100.0%
Altaire bridge	12045200	19.5	SSC	2012–2013	639	3.150	95.8%
above Lake Mills gauge	12044900	25.1	neph	2011–2013	514	3.378	82.5%
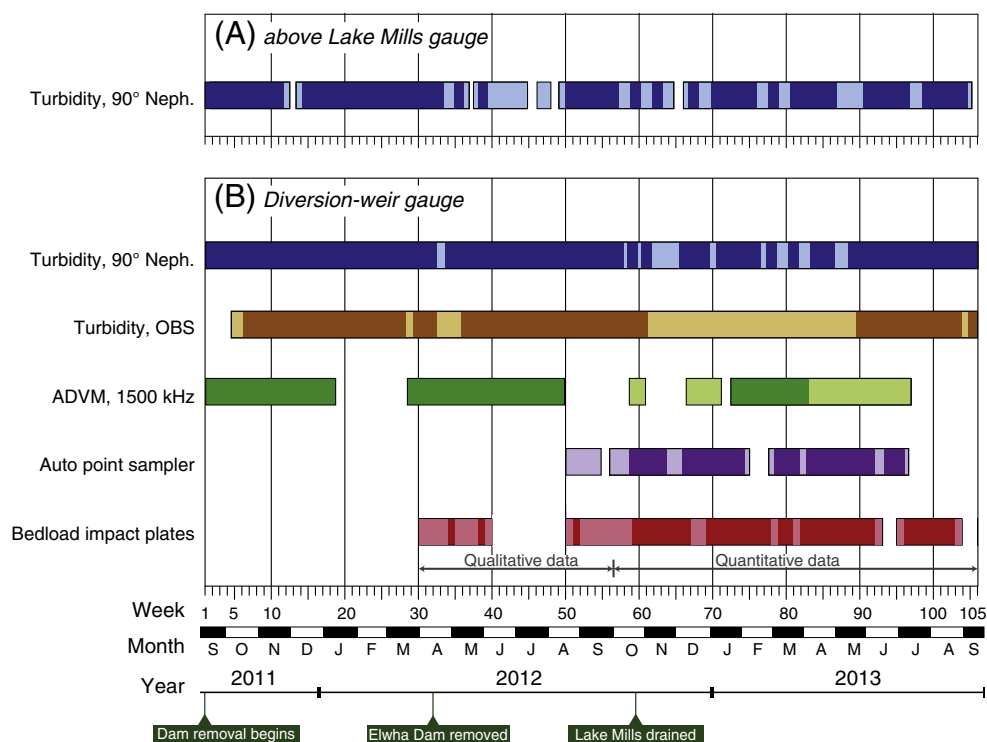
Fig. 2. Timeline showing operation of sediment-surrogate instruments and auto sampler at (A) above Lake Mills gauge (#12044900) and (B) diversion-weir gauge (#12046260) on the Elwha River from 15 September 2011 to 15 September 2013. For each instrument or sampler, darker colors represent >95% utilization for the week and lighter colors represent 5–95% utilization. A gap in the color bars represents <5% utilization. For the bedload impact plates, descriptions of qualitative versus quantitative data collection are given in the text. (For interpretation of the references to color in this figure legend, the reader is referred to the web version of this article.)

the project, some reduction in uncertainty might be justified by calculating the standard error of the mean if the error source were random (Taylor, 1997). Because neither the source of error nor the magnitude of measurement bias are well known, we assumed that uncertainty of the total suspended-sediment load for the full two years of the project was 50%.

3.4. Bedload transport at diversion weir

3.4.1. Gauging bedload using surrogates

We gauged bedload >16 mm at the diversion weir using an array of steel bedload-impact plates (Hilldale et al., 2014) installed in a configuration resembling those constructed in Switzerland and Austria (Bänziger and Burch, 1990; Rickenmann and McArdell, 2007, 2008) and spanning the entire 39-m cross section of the river. Bedload gauging was qualitative in year 1 as the system was refined and improved thus allowing full quantitative bedload gauging for year 2. The collision of larger gravel on the impact plates caused acoustic signals (i.e., impulses) detectable with geophones mounted under the plates, thus enabling the development of a surrogate relation between bedload and impulse frequency applicable to particles >16 mm (Rickenmann and McArdell, 2007, 2008; Hilldale et al., 2014). The system could not directly gauge bedload <16 mm (Hilldale et al., 2014), and other approaches (discussed below) were used to estimate this finer-grained bedload component. Sensor saturation from increased sand in bedload transport has been known to suppress impact frequency (Hilldale et al., 2014; Rickenmann et al., 2014); however, we did not observe detectable saturation in the Elwha River system. The diversion-weir crest was engineered to create near-critical flow conditions over the plates for all but the highest discharges, minimizing localized sedimentation that might otherwise affect impact-plate response.

To calibrate the bedload-impact sensors, physical bedload samples were collected during four separate events from November 2012 to June 2013 using a Toutle River 2 bedload sampler with a 15.2- by

30.5-cm opening and a 1.40 expansion ratio (Childers, 1999). The bedload samples were collected from a raft tethered along the weir crest to allow sampler positioning directly upstream from the impact plates (Hilldale et al., 2014). Because of heavy sediment conditions, 2-mm mesh bags were used on the bedload sampler. Trials with smaller mesh sizes resulted in rapid clogging of the sample bag with observable decreased sample intake efficiency. Even with the 2-mm bags, sizeable volumes of <2-mm particles accumulated in the sample bags and were processed and reported. Because bedload particles <2 mm were not fully trapped in the mesh bags, particle-size distributions from bedload samples are biased and underreport the finer-grained proportion of bedload.

Bedload transport for >16-mm particles, M, in kg/h, was determined using the equation,

$$M = \frac{S}{k_b} \tag{2}$$

where S is the cumulative number of impulses on the impact plate(s) over 1 h and $k_b = 1.17$ is an empirically derived calibration parameter determined using synchronous bedload samples and impact-plate impulses (Hilldale et al., 2014). Integrating the number of impulses per hour allowed the averaging of temporal variations in impulse frequency that we observed with data from the Elwha River. Studies on other rivers indicate similar averaging time periods necessary to compensate for bedload variability (Einstein, 1937; Gomez et al., 1990; Gomez and Troutman, 1997; Habersack, 2001).

In year 1 of the project, threshold voltages on the geophones were set in a fashion that precluded application of a bedload-surrogate relation. However, when operational, geophones recorded the number of impulses per hour, which we interpreted to be a qualitative indication of active >16-mm bedload in year 1. In year 2, the bedload-surrogate relation (Eq. (2)) was developed, allowing us to gauge bedload except during periods of computer-system failures or other issues (Fig. 2). To

estimate M during down periods, we used a bedload-discharge rating of the form,

$$M = AQ^b \tag{3}$$

where A and b are empirical parameters. For a given down period, we calculated A and b by interpolating from valid data collected before and following the down period.

We estimated bedload in the size class from very fine to medium gravel (2–16 mm) using the measured proportional ratio of coarse-grained (>16 mm) to finer-grained (2–16 mm) material from the bedload samples and by linearly interpolating between sample periods. The sediment-size distributions from sampled data were used to determine monthly proportions of the two size ranges throughout year 2, interpolating between data-collection periods and extrapolating beyond data-collection periods at the beginning and end of year 2.

3.4.2. Estimating ungauged bedload

Observations from the Elwha River corridor (East et al., 2015) and coast (Gelfenbaum et al., in this volume) as well as our observations during bedload sampling indicated sizeable <2-mm bedload transport occurring for much of the study period. In order to estimate ungauged bedload (including all bedload from year 1), comparative studies and data sets were queried to assess typical bedload-to-total-load ratios from other heavy sediment-load rivers in the U.S. Pacific Northwest. Curran et al. (2009) analyzed sediment rating curves for the Elwha River into Lake Mills to estimate that bedload was about 27% of the total load. In the sediment-rich White River of western Washington, which drains the glaciated and recurrently active Mount Rainier volcano, Czuba et al. (2012) took five paired samples from 2010 to 2011, finding that bedload-to-total-load ratios ranged from 7 to 15%. Thirteen paired samples of the Toutle River and North Fork Toutle River in the spring and summer of 1985 showed bedload-to-total-load ratios ranging from 2 to 34% (Hammond, 1989). These samples were collected five years after the major 1980 eruption of Mount St. Helens volcano in the headwaters of the Toutle River system (Lipman and Mullineaux, 1981), and by 1985, total sediment loads on the Toutle River system had decreased relative to loads in the early 1980s (Major, 2004). Based on a long-term sediment-monitoring program, Madej and Ozaki (1996) reported that bedload was 20 to 25% of total load in Redwood Creek, a river draining 730 km^2 in northern coastal California where logging and a series of large floods induced heavy long-term sediment loads of 1.0–1.5 million t/y through the latter half of the twentieth century (Nolan et al., 1995; Warrick et al., 2013). Major et al. (2012) determined that in the first year following the Marmot Dam removal, the bedload-to-total-load ratio was 38% at a gauge 0.4 km downstream from the dam site, 28% at a gauge 9 km downstream from the dam site, and 5–20% at a gauge 10 km upstream from the dam site.
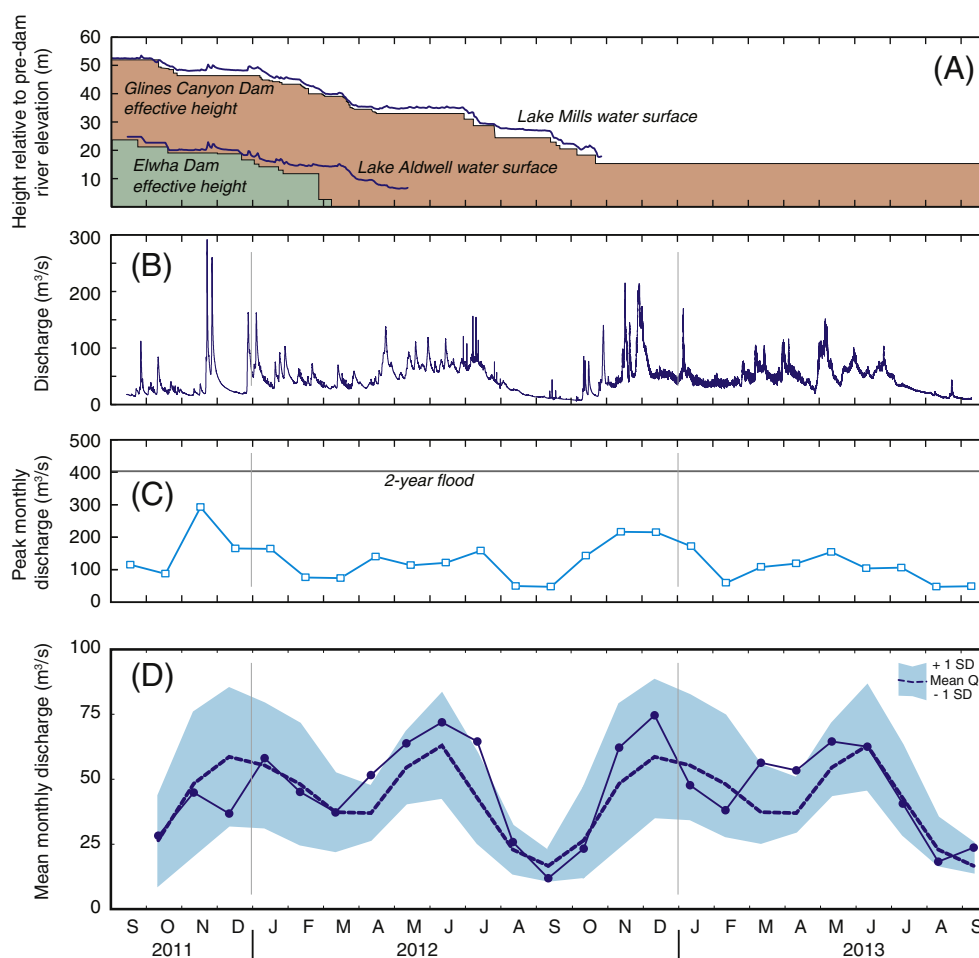

Fig. 3. Chronology of first two years, 15 September 2011 to 15 September 2013, of Elwha River dam-removal project showing (A) progress of lake-level elevation in both reservoirs and effective dam heights, (B) discharge hydrograph, (C) monthly peak flows shown with the 2-year recurrence-interval flood, and (D) mean monthly discharge compared to long-term average. The Elwha Dam structure was completely removed by March 2012, but coffer dams and continued deconstruction activities continued through most of April maintaining a pool in Lake Aldwell until early May 2012. Discharge was measured at McDonald Bridge gauge (#12045500).

We assumed that the bedload-to-total-load ratio applicable at the diversion-weir gauge in year 1 was about 15%. Starting October 2012, the river corridor came under the geomorphic influence of sand-sized and coarser-grained sediment released from Lake Mills (East et al., 2015). We assumed that the bedload-to-total-load ratio in year 2 was about 25%. These estimated bedload values were reported as the total bedload for year 1 of the project, when no other gauged bedload was available. For year 2 of the project, estimates of <2-mm bedload were calculated by subtracting the gauged bedload (i.e., >2 mm) from the estimated total bedload.

3.4.3. Uncertainty of bedload estimates

We estimated that the uncertainty for gauged >16-mm bedload (M) was ±52%, based on the standard deviation of the relative error of the preliminary calibration data. Knowing the implicit uncertainty in bedload sampling (Hubbell and Stevens, 1986; Childers, 1999) and not having independent bedload data to evaluate uncertainty, we assumed that the cumulative uncertainty in reported 2–16-mm bedload data was ±80%. We assumed that the cumulative uncertainty of the total bedload estimates (all size classes) was ±90%.

3.5. Sediment load into Lake Mills

The total sediment load entering Lake Mills during the first two years of the restoration project was calculated using transport equations of Curran et al. (2009). Based on suspended-sediment data collected in 1994–1998 and 2005–2006, Curran et al. determined empirically that daily suspended-sediment load for the Elwha River at the above Lake Mills gauging site was

$$Q_S = 1.08 \times 10^{-5} Q^{4.0}. \tag{4}$$

Using bedload data collected from 1994 to 1997 (Childers et al., 2000), Curran et al. found that daily bedload (Q_B, in tonnes) was

$$Q_B = 1.13 \times 10^{-2} Q^{2.41}. \tag{5}$$

Combining estimates of daily discharge for the Elwha River above Lake Mills with the sediment-discharge relations allowed estimates of total sediment load ($Q_S + Q_B$) into Lake Mills from the upper Elwha River for the first two years of the dam-removal project.

Uncertainty in the estimates of sediment loads into Lake Mills was determined using the adjusted maximum likelihood estimator (AMLE; Cohn, 2005) calculated with the Load Estimator (LOADEST) software package (Runkel et al., 2004). We assumed that the relative uncertainty of discharge was small when compared to the uncertainty associated with the sediment rating curves. The AMLE corrects load estimates caused by transformation bias (Duan, 1983), and LOADEST reports uncertainty of upper and lower load estimates.

Table 2

Suspended-sediment sample data for the water-quality monitoring sites Elwha River at Diversion, near Port Angeles, Washington (#12046260) and Elwha River at Altair Bridge, near Port Angeles, Washington (#12045200). Concentration and percent values are event averages. EWI, Equal width increment; EDI, Equal discharge increment; mg, milligrams; mg/L, milligrams per liter; mm, millimeter; Rkm, river kilometer; n.d. no data.

Sampling method	Sample date	Sample time	Loss on ignition of suspended solids, percent	Suspended-sediment concentration, mg/L	Suspended sediment, < 0.063 mm	Suspended sediment, > 0.063 mm and < 0.5 mm
Samples collected at the diversion weir (#12046260; Rkm 5.1)						
EDI	18-Nov-11	14:16	n.d.	104	99%	n.d.
EWI	22-Nov-11	14:47	n.d.	281	75%	25%
EWI	30-Dec-11	13:32	n.d.	695	92%	8%
EWI	5-Jan-12	12:14	n.d.	443	83%	15%
EWI	5-Jan-12	14:44	n.d.	315	86%	13%
EWI	23-Jan-12	13:23	n.d.	375	89%	11%
EWI	16-Mar-12	12:17	n.d.	363	83%	16%
EWI	16-Mar-12	15:02	n.d.	517	83%	16%
EWI	19-Mar-12	11:00	n.d.	202	93%	7%
EWI	29-Mar-12	11:59	n.d.	1880	87%	13%
EWI	23-Jun-12	15:14	n.d.	408	61%	n.d.
EWI	11-Jul-12	10:21	n.d.	345	74%	n.d.
EWI	11-Jul-12	16:13	n.d.	324	78%	n.d.
EWI	21-Aug-12	13:31	n.d.	44	84%	n.d.
EWI	16-Oct-12	11:53	5%	1550	95%	n.d.
EWI	31-Oct-12	12:43	4%	6570	63%	n.d.
EWI	20-Nov-12	10:36	3%	11,600	39%	n.d.
EWI	4-Dec-12	13:21	3%	9950	47%	45%
EWI	11-Jan-13	13:33	3%	4040	24%	70%
EWI	11-Jan-13	14:21	3%	8800	23%	46%
EWI	13-Mar-13	15:19	4%	12,100	66%	11%
EWI	8-Apr-13	15:58	n.d.	6950	59%	11%
EWI	7-May-13	15:03	4%	6620	69%	13%
EWI	17-May-13	13:50	n.d.	8570	58%	n.d.
Samples collected at Altaire bridge (#12045200; Rkm 19.5)						
EWI	16-Oct-12	15:22	4%	1230	94%	n.d.
EWI	31-Oct-12	16:13	4%	12,600	30%	69%
EWI	20-Nov-12	14:15	3%	14,700	27%	68%
EWI	11-Jan-13	11:50	3%	8600	23%	48%
EWI	13-Mar-13	12:58	4%	16,300	48%	44%
EWI	8-Apr-13	13:42	n.d	7590	51%	37%
EWI	7-May-13	11:36	3%	6410	67%	19%
EWI	7-May-13	12:45	n.d	6490	65%	n.d.
EWI	17-May-13	10:16	n.d	9290	38%	n.d.
EWI	17-May-13	11:03	n.d	6820	51%	n.d.

4. Results

4.1. Dam-removal chronology and hydrology

The dominant processes governing sediment mobilization during dam removal were the dam drawdown activities and the runoff hydrology in the Elwha River. Dam removal commenced in September 2011 with drawdown notching on both dams (Fig. 3). The lake-level elevation of both reservoirs rose and fell as a function of river discharge and hydraulic control of the shrinking dam structures (Fig. 3). On the Elwha Dam, drawdown notching occurred from September through October 2011, bringing the effective dam height from about 24 m down to 19 m. Notching was suspended for most of November and December then resumed from January 2012 through March 2012. Dam height in February was 11.7 m and lowered to 2.6 m in early March 2012. Construction and deconstruction of coffer dams along with removal of the final Elwha Dam structure maintained some semblance of pool impoundment of former Lake Aldwell through early May 2012. From May 2012, Lake Aldwell ceased to exist and trapped sediment was transported downstream. Drawdown notching occurred on Glines Canyon Dam from September 2011 through October 2012 with three distinct hold periods in November–December 2011, May–June 2012, and August–September 2012 (Randle et al., in this volume). The initial Lake Mills water level of 52 m fell to 46.4 m by the end of October 2011. From January through middle April 2012, the effective dam height was lowered from 46.4 to 33.3 m. During July 2012, drawdown notching lowered the dam height to 24.4 m. Notching actions in September and October 2012 lowered the dam height to 15.3 m. By October 2012, the remnant Lake Mills reservoir ceased to exist and coarse-grained sediment started spilling over the top of the lowered Glines Canyon Dam structure sharply increasing SSC, bedload, and downstream geomorphic response (East et al., 2015). From November 2012 to September 2013, dam-removal activities were held to allow incision and stabilization of the sediment deposit in the former Lake Mills.

The climate during the study period was colder and wetter than normal, and runoff was greater than normal with only modest peak flows. The average flow in the Elwha River during the study period, as measured at the McDonald Bridge gauge, was 107% of the mean annual discharge in year 1 and 108% of the mean annual discharge in year 2. During the study period, winter and summer runoff was near normal (Fig. 3). Both spring snowmelt seasons, however, had above-normal
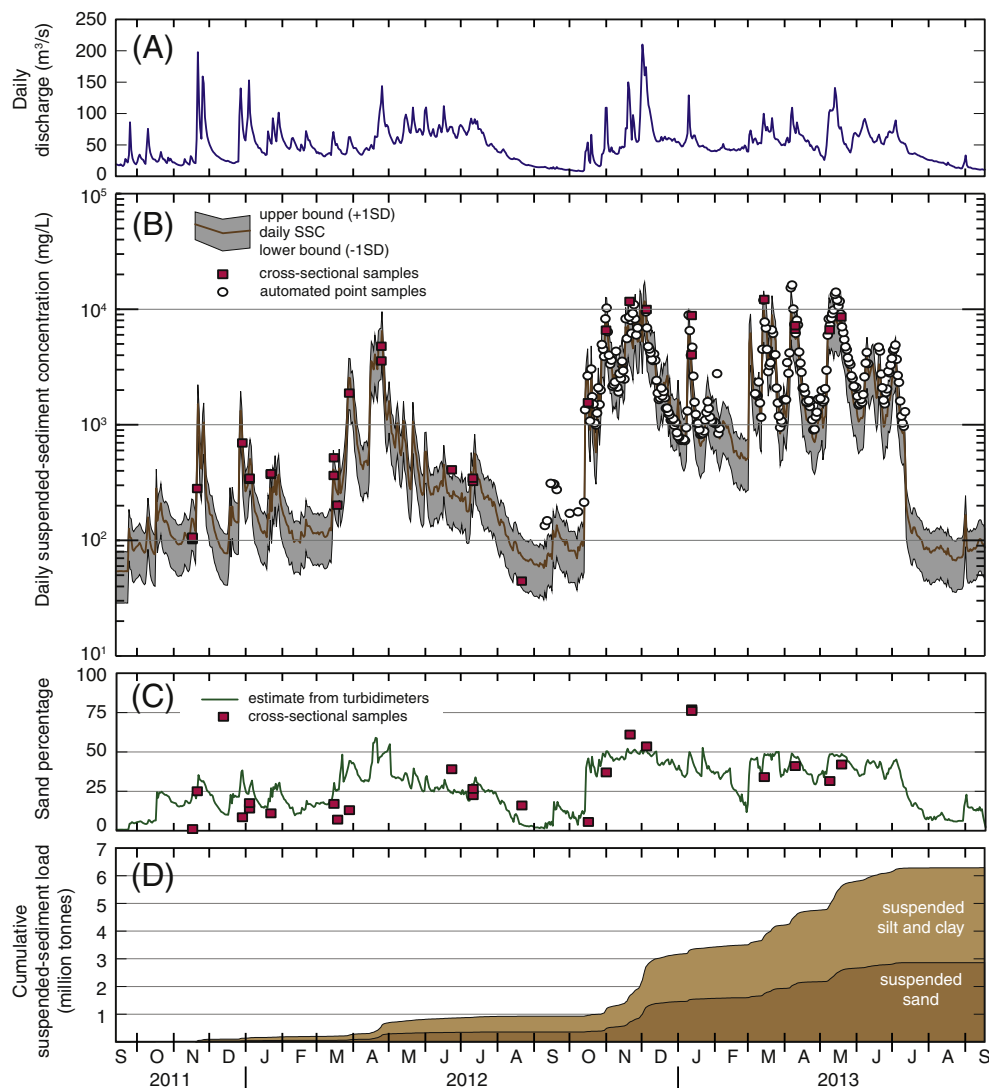

Fig. 4. (A) Daily discharge at McDonald Bridge gauge (#12045500), (B) surrogate-calculated suspended-sediment concentration, (C) sand percentage of suspended-sediment concentration, and (D) cumulative suspended-sediment load in the lower Elwha River as measured at the diversion-weir gauge (#12046260) from 15 September 2011 to 15 September 2013. In panel (B), one standard deviation uncertainty for suspended-sediment concentration is shown as the gray region, and cross-sectional and automated-point-sample measurements are plotted for comparison.

runoff caused by spring rains and heavy snowpack: 169% of normal as of 1 May 2012 and 135% of normal as of 1 May 2013 (NRCS, 2014). Despite the wet weather, peak flows during the study period were small. The largest peak-flow event was 292 m³/s on 23 November 2011 before substantial release of sediment from either reservoir, and all other monthly peak flows were <215 m³/s (Fig. 3C).

4.2. Suspended-sediment concentration

Physical samples indicated the river carried larger SSC values during periods of increased discharge with greater sand fractions typically occurring following dam notching activity. Cross section SSC samples collected at the diversion weir ranged from 7 to 12,200 mg/L, and SSC of bias-adjusted SSC from point samples ranged from 134 to 16,200 mg/L (Table 2). The mean sand fraction for diversion-weir cross section samples was 31% compared with 7% for a population-representative subgroup of point samples. The contrast between cross section and point sample SSCs, as well as the percentage of sand, demonstrated the heterogeneity of suspended sand in the channel. Temporal patterns in sand percentage were also evident with lower relative sand percentage before March 2012 when Lake Mills and Lake Aldwell contained enough reservoir capacity to trap coarser-grained suspended sediment. Relative sand percentage increased in the summer of 2012, presumably in response to the complete removal of the Elwha Dam and the release of Lake Aldwell sediment. Sand percentage rose from November 2012 through January 2013 to about 75% of the total suspended load (Table 2). This higher sand concentration was likely associated with the initial flush of sediment from former Lake Mills.

Daily mean SSC derived from 15-minute sediment-surrogate data ranged from 54 to 6490 mg/L in the first year and from 67 to 11,700 mg/L in the second year. The largest 5-day median SSCs were 4600 mg/L from 23 to 27 April 2012 and 9850 mg/L from 29 November to 2 December 2012 in the first and second years, respectively. Daily SSC values at the start of the project were relatively small until 25 September 2011, when the first rise in discharge above 50 m³/s increased SSC to about 100 mg/L (Fig. 4; Appendix C). From October to early March in the first year of the project, daily SSC values were generally between 100 and 300 mg/L, except during three distinct periods of higher flow in late November, late December, and January, when SSC values commonly were 500–1000 mg/L and SSC rose above 1000 mg/L for a few days. In year 1, SSC values exceeded 500 mg/L 17% of the time and exceeded 1000 mg/L 9% of the time. The percentage of sand-sized particles in suspension was generally <25% through early March 2012. Starting about 16 March 2012, SSC values increased consistently above 400 mg/L with sand-percentage values between 25 and 60% until the middle of May 2012. Suspended-sediment transport was particularly pronounced in the latter half of April 2012 with SSC values from 3000 to 6500 mg/L and sand-percentage values near 50% (Fig. 4). This marked increase in daily SSC and sand percentage coincided with the loss of Lake Aldwell as a sediment-transport capacitor and the release of coarse-grained sediment in suspension to the lower river. In May, SSC dropped to about 1000 mg/L then progressively decreased to about 250 mg/L by late June 2012. The sand fraction also declined over this same time frame to about 25%. Late-summer low flow and cessation in dam-drawdown activity allowed the SSC to drop below 100 mg/L with corresponding sand fractions <5% (Fig. 4).

Year 2 of the project brought increased daily SSC and sediment transport. The shrinking Lake Mills reservoir and increased river discharge from seasonal rainfall released copious volumes of sediment to the river resulting in marked increases in SSC and sand percentage. Starting about 15 October 2012, SSC at the diversion weir rose above 1000 mg/L and sand fraction increased above 40% (Fig. 4). A series of storms and heavy rainfall from 18 November 2012 to 12 December 2012 resulted in sustained high river flows with daily SSC values above 5000 mg/L and a maximum value of 11,700 mg/L. Except for an isolated storm on 9 January 2013, reduced flows from December 2012
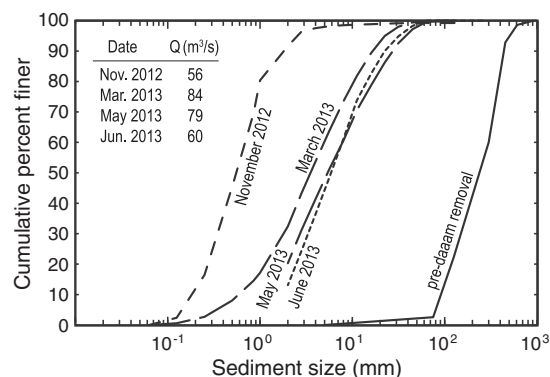

Fig. 6. Particle-size distribution of bedload samples taken at diversion-weir gauge between November 2012 and June 2013. Comparative pre-dam removal sample is based on a bed-material sample of the Elwha River near the diversion weir.
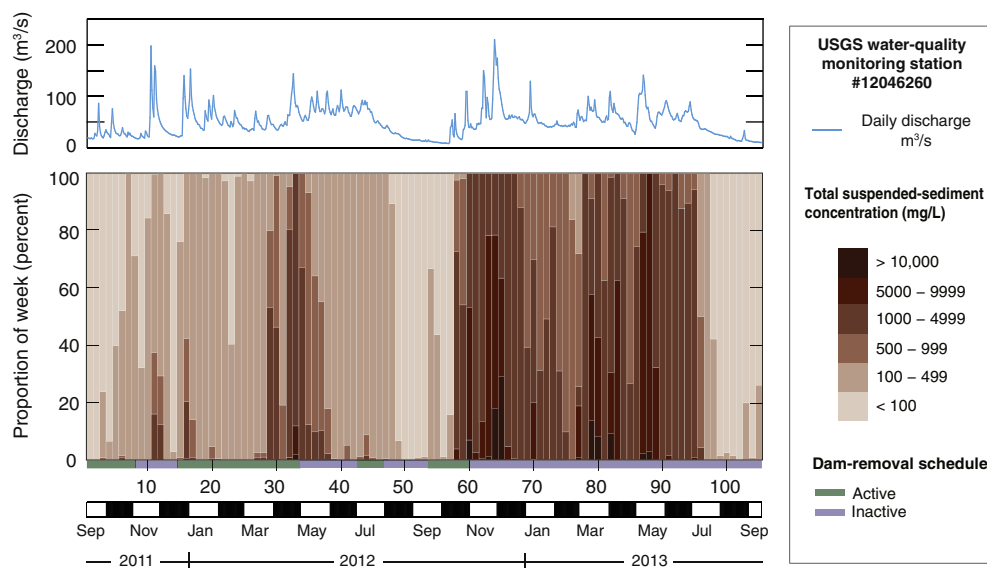

Fig. 5. Graph showing suspended-sediment concentration bins as a proportion of each week during the first two years of dam removal on the Elwha River.

Table 3
Summary of physical bedload samples collected using a modified Helley–Smith bedload sampler (Toutle River 2) with a 2-mm mesh bag.

Sample dates	Daily discharge (m³/s)	Daily SSC (mg/L)	Daily bedload >2 mm (tonnes/day)	Median particle size (mm)	Bedload fraction <2 mm	Bedload fraction 2–16 mm	Bedload fraction >16 mm
27–28 Nov. 2012	54.8; 57.6	5230; 5300	198; 261	0.6	91.6%	7.2%	1.2%
13–15 Mar. 2013	100; 83.6; 72.9	9820; 8460; 8080	2870; 3120; 2820	3.5	32.4%	57.0%	10.6%
14–15 May 2013	102; 80.4	7510; 7340	5340; 4140	5.4	20.3%	58.5%	21.2%
12–13 June 2013	60.6; 55.7	3280; 3380	2490; 1790	5.9	13.1%	69.5%	17.4%

through February 2013 allowed SSC to decrease to <500 mg/L and sand percentage dropped to below 25% (Fig. 4). Increased rainfall runoff starting in March 2013, combined with snowmelt, ushered in a series of modest high-flow events through July of about 100 m³/s; SSC values typically ranged between 1000 and 10,000 mg/L, rising occasionally above 10,000 mg/L, and the percent sand rose to near 50%. By late July 2013, daily discharge dropped below 50 m³/s and SSC decreased to about 100 mg/L (Fig. 4). Except for one small high-flow event on 30 August 2013, SSC values remained between 50 and 100 mg/L in the late summer, with sand-percentage values about 10% for the remainder of the study period until 15 September 2013. In year 2, SSC values exceeded 500 mg/L 74% of the time, exceeded 1000 mg/L 59% of the time, and exceeded 10,000 mg/L 0.8% of the time.

Plotting the proportion of time spent in different SSC-by-concentration bins during any given week of the study period allowed a graphical interpretation of how ecological systems in the Elwha River might respond (Fig. 5). Low SSC conditions (SSC values < 100 mg/L for more than about 80% of the week) occurred during the first 4 weeks of the study period and for about 6–8 weeks in late summer of both 2012 and 2013 (Fig. 5). Moderate SSC conditions (SSC values between 100 and 1000 mg/L) prevailed from October 2011 to August 2012, during year 1 of the study period. High SSC conditions (SSC > 1000 mg/L) also occurred for about 5 weeks in the spring of year 1 upon release of Lake Aldwell coarse-grained sediment to the lower river. In year 2, high SSC conditions prevailed from October 2012 to July 2013, with a few weeks from November to December 2012 and March 2013 when SSC values were above 10,000 mg/L for a substantial proportion of time (Fig. 5).

4.3. Suspended-sediment load

During the first two years following dam removal, 6,300,000 ± 3,200,000 t of suspended-sediment load were transported past the diversion-weir gauge (Fig. 4; Appendix C). About 3,400,000 t of this

load was silt and clay and about 2,900,000 t was sand. As expected, the timing of sediment delivery was influenced by the pace of dam de-construction, which controlled sediment availability, and hydrologic factors, which affected the transport capacity of the river. The total suspended-sediment load in year 1 of the study was 930,000 t (570,000 t silt- and clay-sized and 360,000 t sand-sized), predominantly reflecting the release of sediment from the former Lake Aldwell (Randle et al., in this volume) and the continued shrinking effectiveness of Lake Mills as a sediment trap. A sixfold increase in sediment loads was observed between year 1 and year 2 with 5,400,000 t of suspended sediment transported past the diversion-weir gauge in year 2 (2,900,000 t silt- and clay-sized and 2,500,000 t sand-sized). In year 1, 25% of suspended-sediment load (230,000 t) was transported in 5 days (23–27 April 2012) during a single runoff event in which discharge peaked at 155 m³/s (Fig. 4). In year 2, 12% of annual suspended-sediment load (630,000 t) was transported in the largest 5-day runoff (29 November–3 December 2012) when the discharge peaked at 235 m³/s. Of the 6,300,000 t of suspended-sediment load gauged during the study period, 15% transported in year 1 and 85% transported in year 2.

4.4. Gauged bedload

Both bedload samples and impact plates indicated that bedload transport loosely tracked temporal SSC trends. Gravel first arrived in April 2012 with the complete removal of the Elwha Dam and the substantive bedload release from the former Lake Mills in October 2012. Bedload samples taken on 27–28 November 2012 had a median grain size of 0.6 mm (Fig. 6; Table 3) and showed the high proportion of sand-sized bedload just after the sediment release from former Lake Mills. Starting March 2013, bedload caliber coarsened, and by May and June 2013, bedload was mostly gravel (Fig. 6; Table 3). Qualitative bedload data from year 1 confirmed that until late April 2012, negligible
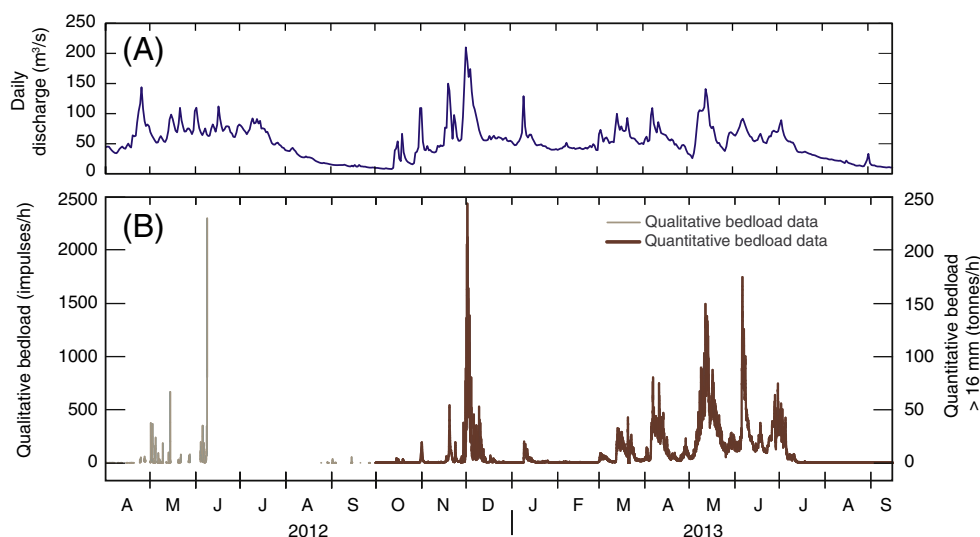

Fig. 7. (A) Daily discharge measured at McDonald Bridge gauge (#12045500) and (B) transport of bedload >16 mm for year 2 of the Elwha River dam-removal project. Qualitative data of bedload transport from part of year 1, based on the number of impact-plate impulses per hour, are also shown.
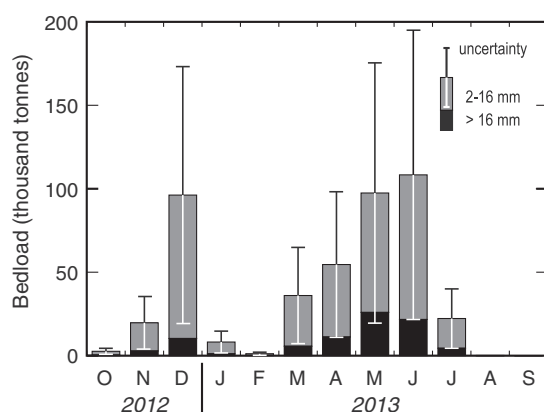
Fig. 8. Monthly bedload for 2–16-mm and >16-mm size classes in the Elwha River at the diversion-weir gauge (#12046260) for year 2 of the dam-removal project. Uncertainty of total bedload >2 mm is one standard deviation.

quantities of gravel were transported (Fig. 7). In late April 2012, impact-plates impulses from >16-mm particles started. From 1 May to the middle of June 2012, bedload impulses were numerous, reflecting release of bedload from the former Lake Aldwell after full removal of the Elwha Dam. Equipment malfunctions from late June through middle August 2012 prevented assessments of bedload; however, occasional impact-plate impulses occurred in late August and September 2012, indicating that modest gravel transport was detectable in the late summer of year 1 despite the reduced flows.

Impact-plate impulses in year 2 indicated modest transport beginning around 14 October 2012. Bedload increased 31 October 2012 with a high-flow event (Fig. 7; Appendix C). Sustained bedload transport of substantial magnitude started on 17 November 2012 and continued through late December (Fig. 7), with as much as 24,700 t/d of >2-mm bedload transporting in early December, the largest daily bedload rate measured during the study period. Monthly bedload totals increased from October through December 2012; and in December, 96,000 t of >2-mm bedload transported past the diversion-weir gauge (Fig. 8), about 90% (86,000 t) of which was 2–16 mm. Because of reduced runoff, gauged bedload in January and February was relatively small—less than 10,000 t each month. Higher discharge from March through June 2013 increased bedload transport, concurrent with larger runoff. The monthly gauged bedload in June 2013 was about 110,000 t, the largest monthly total measured at the gauge. By June 2013, 2–16-mm bedload transport was about 86,000 t, and the >16-mm proportion of bedload was 22,000 t, a twofold increase relative to December 2012. This increase of the coarsest fraction of bedload likely reflected arrival of coarse-grained material from former Lake Mills; we found that >16-mm bedload in May and June 2013 (48,000 t) was 3.5 times the >16-mm bedload in November and December 2012 (13,000 t). Monthly gauged bedload dropped to about 22,000 t in July 2013, then below 1000 t for the rest of the study period to 15 September 2013 (Fig. 8).

Bedload transport effectively ceased from late July to September 2013. For year 2 of the project, >16-mm and 2–16-mm bedload were 84,000 t and 363,000 t, respectively, for a total of 450,000 ± 360,000 t of gauged bedload past the diversion-weir gauge.

4.5. Ungauged sediment load and above Lake Mills turbidity

Scaling to gauged suspended-sediment load and based on comparative studies, we estimated that the total bedload in year 1 was about 160,000 t. This value is reported as the total year-1 bedload for all size classes (Table 4). In year 2, we estimated that the total bedload, based on the assumed bedload-to-total-load ratio, was about 1,800,000 t. The gauged bedload was 450,000 t; therefore, the year-2 bedload of particles <2 mm was estimated at 1,300,000 t. The two-year total of ungauged bedload during the project was estimated to be 1,500,000 ± 1,400,000 t.

Combining the sediment-load measurements and estimates at the diversion weir, the summation of all loads (including the suspended-sediment load, the gauged bedload, and the ungauged bedload) yielded a total Elwha River sediment load of 1,100,000 t in year 1 of the project and 7,100,000 t in year 2. The total sediment load during the study period, from 15 September 2011 to 15 September 2013, was 8,200,000 ± 3,400,000 t (Table 4).

Using the sediment rating curves of Curran et al. (2009), we estimated total sediment loads of about 38,000 t in year 1 and 45,000 t in year 2 flowing into the Lake Mills reach from the upper Elwha River (Table 5). The estimated sediment load into Lake Mills during the first full two years of the dam-removal project totaled 83,000 t (uncertainty range: 60,000–110,000 t). Turbidity values from the above Lake Mills gauge qualitatively confirmed that SSC values entering the project area were smaller than values downstream. Data from the diversion-weir gauge compared to data from the above Lake Mills gauge showed that downstream turbidities were 10 to almost 1000 times greater than upstream turbidities (Fig. 9). Turbidity ratios also grouped into five distinct time periods of enhanced or reduced relative magnitude. We discuss these time periods below.

5. Discussion

The Elwha River sediment loads downstream from the dam-removal project (1,100,000 t in year 1 and 7,100,000 t in year 2) were 3 and 20 times larger than the long-term Elwha River mean annual sediment load (340,000 ± 80,000 t/y). The year-2 sediment load was also greater than the roughly 6 million t of annual sediment discharged from all rivers flowing into Puget Sound of western Washington (Czuba et al., 2011b) and about one-third the annual sediment discharge of British Columbia's Fraser River (20 Mt/y; Church and Krishnappan, 1998). The Elwha River sediment discharge in year 2 was comparable to the estimated 10-Mt sediment discharge of the Columbia River (Meade and Parker, 1985), the largest river flowing into the Pacific Ocean from North America (Kammerer, 1990), although dams retain about 60% of

Table 4
Sediment loads measured and estimated at the diversion-weir gauge (#12046260) during the first two years of the dam-removal project, from 15 September 2011 to 15 September 2013. Column and row entries may not add exactly because of rounding. [n/m — not measured].

	Suspended-sediment load, silt and clay (tonnes)	Suspended-sediment load, sand (tonnes)	Total suspended-sediment load (tonnes)	Gauged bedload; 2–16-mm particles (tonnes)	Gauged bedload; >16-mm particles (tonnes)	Total gauged bedload (tonnes)	Estimated ungauged bedload (tonnes)	Total sediment load (tonnes)
Year 1	570,000	360,000	930,000	n/m	n/m	n/m	160,000	1,100,000
Year 2	2,900,000	2,500,000	5,400,000	360,000	84,000	450,000	1,300,000	7,100,000
2-year total (15 Sept 2011–15 Sept 2013)	3,400,000	2,900,000	6,300,000	360,000	84,000	450,000	1,500,000	8,200,000
Uncertainty—lower bound (2-year total)			3,200,000			90,000	150,000	4,800,000
Uncertainty—upper bound (2-year total)			9,400,000			800,000	2,900,000	12,000,000

Table 5

Sediment loads entering the restoration project area into the former Lake Mills from upstream reaches of the Elwha River during the first two years of the dam-removal project, from 15 September 2011 to 15 September 2013.

	Suspended-sediment load (tonnes)	Bedload (tonnes)	Total load (tonnes)
Estimated sediment load into Lake Mills—15 September 2011 to 15 September 2013			
Year 1	34,000	4000	38,000
Year 2	41,000	4000	45,000
2-year total	75,000	8000	83,000
Uncertainty—lower bound (2-year total)	55,000	5600	60,000
Uncertainty—upper bound (2-year total)	100,000	11,000	110,000

the natural Columbia River sediment load (Naik and Jay, 2011). For comparison, the mean-annual discharges of the Fraser and Columbia Rivers are 90 and 175 times that of the Elwha River.

Gauging on the Elwha River gave us insight into the temporal patterns of sediment released from both reservoirs. Model predictions indicated that one-third to one-half the total trapped sediment would mobilize in the first 4–7 years following dam removal (Randle et al., 1996; Konrad, 2009; Czuba et al., 2011a). Uncertainty in sediment gauging as well as uncertainty in bulk density of reservoir sediment make comparisons of gauged sediment loads to model predictions imprecise, but direct volume-change measurements by Randle et al. (2015-in this volume) indicated that of the 21 ± 3 million m^3 of trapped sediment behind both dams, roughly 7 million m^3, or 33%, transported downstream in the first two years. Of this total, 16% and 84% transported in years 1 and 2, respectively, a ratio essentially identical to the proportion of suspended-sediment loads gauged at the diversion weir in years 1 and 2 (Table 4). Notably, Randle et al. (2015-in this volume) found 36% of the total Lake Mills sediment evacuated in a single year (year 2), which is generally faster than model predictions. The efficiency of sediment transport from Lake Mills was also remarkable given the relatively muted peak-flow hydrology of year 2 (Fig. 3).

Analysis of sediment transport as a function of discharge shows that erosion and sediment mobilization from the former reservoirs was, at times, substantive during low and moderate flows. Major (2004) found, when plotting SSC against Q^* (the ratio of instantaneous discharge to mean annual discharge), that rivers draining post-eruption Mount St. Helens carried significant SSC during low flows (i.e., discharges less than
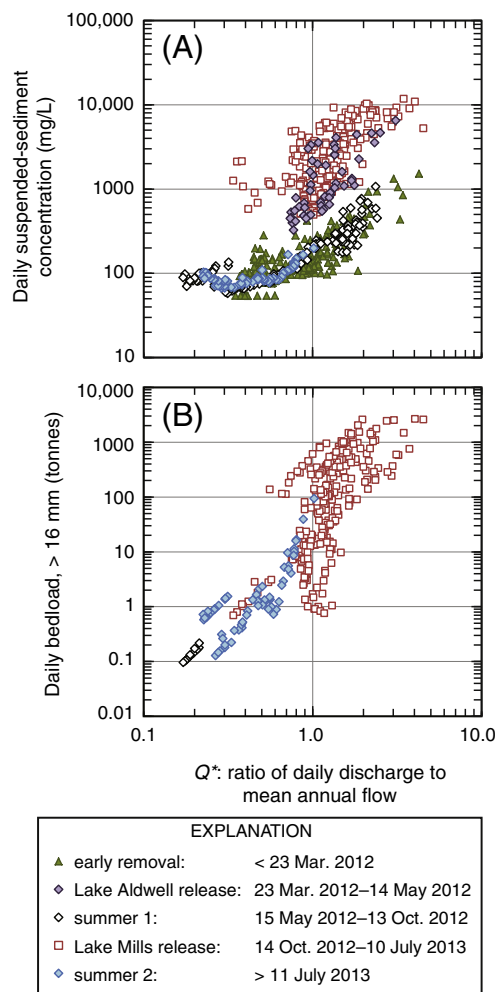

Fig. 10. (A) Daily suspended-sediment concentration, as determined from sediment-surrogate instruments, plotted against daily discharge normalized to mean annual flow, Q^*. (B) Daily bedload >16 mm as determined from bedload-surrogate impact plates, plotted against daily discharge normalized to mean annual flow.
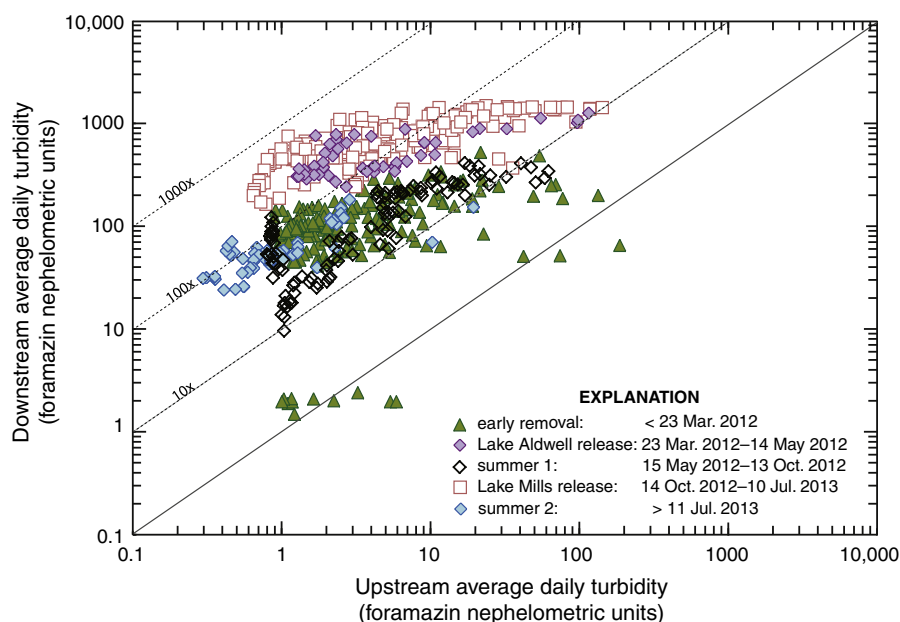

Fig. 9. Daily nephelometric turbidity data measured downstream from the dam-removal project site at the diversion–weir gauge (#12046260) plotted versus turbidity measured upstream from the dam-removal project at the above Lake Mills gauge (#12044900).

mean annual flow). Plotting daily SSC against Q^* for the Elwha River, we also found for certain time periods relatively large SSC values ranging from 100 to 10,000 mg/L for Q^* values from 0.2 to 5 (Fig. 10). The Elwha River SSC data also clustered in two populations with a notable gap: one group of larger concentration values ranging from 1000 to 10,000 mg/L and a second smaller-concentration group with SSCs about an order of magnitude lower for comparable Q^* values (Fig. 10). Similarly, the >16-mm bedload was plotted against Q^*, but daily bedload data did not show a gap between time periods and seemed instead to follow a consistent bedload-to-discharge rating curve (Fig. 10B). Further refinement of the SSC data by date revealed three periods of reduced SSC (early removal, summer 1, and summer 2) and two periods of increased SSC (Lake Aldwell release and Lake Mills release). The near-constant SSC values for $Q^* < 0.35$ ($Q < 15\ \mathrm{m^3/s}$) were likely an artifact of the surrogate regression model; we believe that actual SSC values in the river decreased with $Q^* < 0.35$ instead of remaining constant.

We attribute periods of enhanced SSC to active lateral erosion of the river into loose, unconsolidated sediment of the former reservoirs. We attribute periods of reduced SSC to either suppressed lateral erosion during summer low flow or to the sediment-trapping influence of extant reservoirs. Plotting the chronology of ratios of SSC to Q^* and bedload to Q^* illustrates changing sediment-transport conditions (Fig. 11). The early removal period, when silt and clay were released from both dam sites but sand and gravel were retained in the shrinking reservoirs, resulted in moderate SSC to Q^* ratios. These ratios rose to about 1000 during the two months of the Lake Aldwell release, when about 600,000 t of sediment was transported from the former Lake Aldwell after complete removal of the Elwha Dam. During the Lake Aldwell release, SSC was directly proportional to Q^* reflecting river incision, channel widening, and downstream transport of the Lake Aldwell sediment. Sediment transport during the Lake Aldwell release period is consistent with conceptual models of reservoir evolution following dam
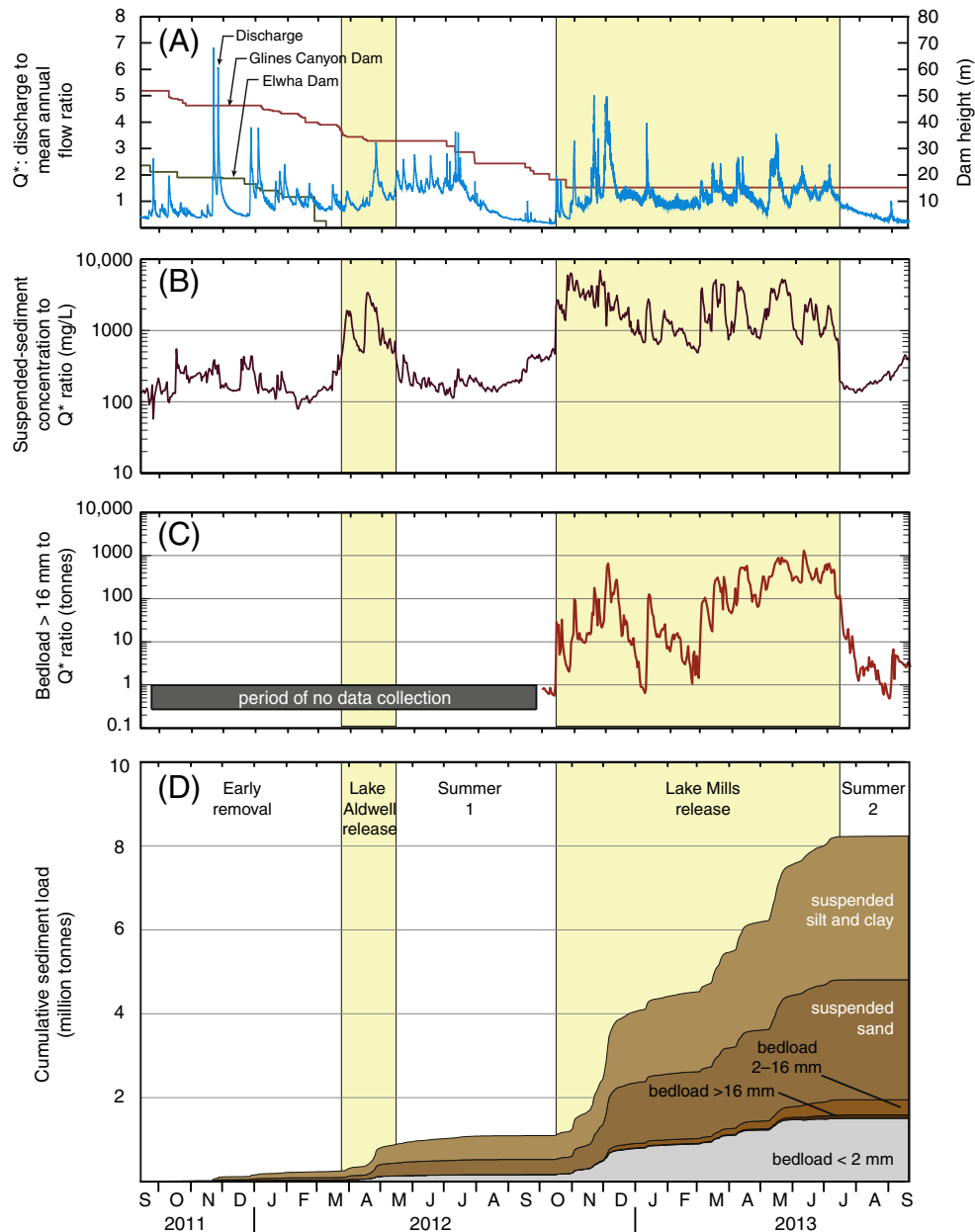
Fig. 11. Graphs showing (A) Elwha River discharge, measured at the McDonald Bridge gauge (#12045500), normalized against the long-term mean annual flow, Q^*, and the dam-removal chronology; (B) the ratio of suspended-sediment concentration to Q^*; (C) the ratio of bedload >16 mm to Q^*; and (D) the cumulative suspended-sediment load and bedload during the first two years of dam removal on the Elwha River. All sediment data were measured at the diversion-weir gauge (#12046260). Also shown are the five distinct sediment-delivery periods identified during the first two years of the project.

removal and subsequent release of sediment downstream (Doyle et al., 2002, 2003b; Pizzuto, 2002), and is similar to transport conditions following removal of Marmot Dam (Major et al., 2012). With decreasing discharge in the summer-1 period, erosional processes in the former Lake Mills subsided and downstream sediment transport decreased (Fig. 4B). Starting in October 2012 with increased discharge and the arrival of heavy sediment loads from the former Lake Mills, SSC to Q^* ratios rose to 1000 or higher for 9 months reflecting near continuous transport of both SSC and bedload (7.1 Mt total) past the diversion-weir gauge (Fig. 11D). During the Lake Mills release, SSC was proportional to Q^* but at greater magnitudes than SSCs during the Lake Aldwell release. Webcam imagery of the former Lake Mills reservoir during the Lake Mills release (Erdman Video Systems, 2013) confirmed a correlation between increased downstream SSC and active lateral erosion in the reservoir (Randle et al., in this volume). On 11 July 2013, the SSC to Q^* ratio dropped to about 200, and only 17,000 t of material transported in the summer-2 period. Webcam imagery from the summer-2 period showed a cessation of lateral erosion, a stabilization of the river within its channel, likely armoring of the channel bed, and a marked decrease in turbidity.

Bedload data at the diversion weir indicated that downstream bedload was not immediately coupled to lateral erosion in the Lake Mills reservoir. The bedload to Q^* ratio showed an increase during the Lake Mills release period and decrease in July 2013; but in contrast to the SSC signal, the bedload data showed more magnitude variability tied to discharge (Fig. 11C) and a consistency with a bedload-to-discharge rating curve (Fig. 10B). In addition, bedload for a given discharge was larger at the end of the Lake Mills release period than at the beginning of the period, particularly for the >16-mm size class, likely reflecting the later arrival of the coarsest component of bedload from Lake Mills. The bedload arriving at the diversion weir in May and June 2013 was greater volumetrically and substantively coarser than the bedload measured in November and December 2012, despite the smaller peak discharge values. While lateral erosion into alluvial deposits resulted in SSC increases that translated far downstream quickly, coarse sand and gravel material added to the channel at Lake Mills was subject to bedload-transport processes that required weeks and months to translate 15 km to the diversion weir as a bed-material sediment pulse.

Notably, large volumes of sediment were transported from both reservoirs despite the relatively benign peak-flow hydrology. The largest flow during the Lake Mills release was 215 m³/s in November 2012, about half the discharge of the 2-year event. For weeks during the Lake Mills release, Q^* was 1.0 or less and yet the SSC to Q^* ratios remained generally 1000 or greater. Webcam imagery indicated that lateral erosion continued during these modest flows contributing sediment to the river channel in a near continuous fashion. For comparison, we estimated that the muted peak-flow hydrology transported only about 83,000 t from the watershed into Lake Mills for the two-year study period, just 12% of the long-term mean sediment discharge.

6. Conclusions

Two years into the largest dam-removal project in U.S. history, the Elwha River has transported 8,200,000 ± 3,400,000 t of total sediment (suspended load and bedload) downstream of the Elwha Dam, with 1,100,000 and 7,100,000 t transporting in years 1 and 2, respectively. During the study period, the discharge in the Elwha River was greater than normal (107% in year 1 and 108% in year 2); however, peak flows were relatively benign. We estimated the total 2-year sediment load into Lake Mills from the upper watershed was only 83,000 t, 12% of the long-term sediment load of 340,000 ± 80,000 t/y. The largest peak discharge of the project occurred 23 November 2011 (292 m³/s) when both reservoirs were retaining sediment. The largest peak flow when both dams were releasing sediment was <215 m³/s, nearly half the 2-year peak-flow event (400 m³/s) for the Elwha River. Despite

these muted peak flows, about 33% of the total sediment trapped in both reservoirs mobilized, and 36% of the sediment in the former Lake Mills reservoir transported in a single year (year 2 of the project). The total sediment discharge of the Elwha River in year 2 of the project equaled the total annual sediment discharge by all rivers flowing into Puget Sound and was comparable to the 10 Mt/y sediment discharge of the Columbia River.

Comparing suspended-sediment concentration to discharge, we found five distinct sediment-transport periods. The early removal (before 23 March 2012), the summer-1 (15 May 2012 to 13 October 2012), and the summer-2 (after 11 July 2013) periods were characterized by reduced overall sediment transport. In contrast, the Lake Aldwell release (23 March 2012 to 14 May 2012) and Lake Mills release (14 October 2012 to 10 July 2013) periods were characterized by marked increases in sediment delivery likely associated with enhanced lateral erosion and sediment transport from the former Lake Aldwell and Lake Mills sediment reservoirs. Sediment transport was greatest when flows increased just after drawdown notching at one or both dams enabled erosion and active transport from the former reservoirs. Suspended-sediment concentrations exceeded 1000 mg/L 9% of the time in year 1 and 59% of the time in year 2, a marked increase that could have important implications for ecological systems in the river corridor. Turbidity values measured downstream of the project were 10 to almost 1000 times those measured upstream of the project.

The largest suspended-sediment concentrations in year 1 occurred from March to May 2012 after final removal of the Elwha Dam. In year 2, sustained high suspended-sediment concentrations lasted from October 2012 to July 2013. During the study period, a total of 6,300,000 ± 3,200,000 t of suspended-sediment load transported past the diversion-weir gauge, with 3,400,000 t silt and clay and 2,900,000 t sand. Of the total suspended-sediment load, 16% (930,000 t) transported in year 1 and 84% (5,400,000 t) transported in year 2.

Bedload was not quantified in year 1, but impact-plate impulses indicated that bedload increased with higher flows in May and June 2012, just after the complete removal of the Elwha Dam and the release of bed material from the former Lake Aldwell. After the release of sediment from the former Lake Mills in year 2, bedload at the diversion weir increased with higher flows in November and December 2012, but more bedload transported from March to June 2013. Bedload increased in magnitude and coarsened through year 2, a trend we attributed to the time required for the bed-material pulse to translate the 15 km from Lake Mills to the diversion weir. In year 2 of the project, bedload transport >2 mm was 450,000 ± 360,000 t, with the >16-mm fraction of 84,000 t and the 2–16-mm fraction of 360,000 t. The proportion of bedload or bed-material transport of sand-sized particles and smaller (i.e., <2 mm) could not be measured or gauged using available techniques; yet, observations and sediment-budget calculations indicated this ungauged bedload was sizeable. We estimated that the total ungauged fraction of <2-mm bedload was 1,500,000 ± 1,400,000 t; 160,000 t in year 1 and 1,300,000 t in year 2.

Appendix A. Discharge-calculation techniques

Stage was measured every 15 min in the Elwha River at USGS streamflow-gauging station #12045500 (Elwha River at McDonald Bridge) using either a stilling well, pressure transducer, or noncontact radar sensor as conditions changed (Fig. 1, Table 1). Discharge at the McDonald Bridge gauge was calculated using a stage-discharge rating consistent with USGS streamflow-gauging protocol (Rantz, 1982). Until 1 November 2012, the stage sensor at the McDonald Bridge gauge was located in a 4-m deep pool constrained by lateral bedrock and hydraulically controlled by a boulder bar located about 100 m downstream. Before dam removal, geomorphic changes in the reach were minimal requiring minor adjustment to the stage-discharge rating. After 1 November 2012, the gauging site was subject to periods of rapid fill and incision as bed material transported past the gauging site (East et al., 2015).

Uncertainty of reported discharge data is a function of the quality of a given discharge measurement, stability of the stage-discharge relation, and the measured stage reading (Rantz, 1982). Following USGS protocol, the uncertainty of the reported discharge data from September 2011 to October 2012 was estimated to be 5%. From 1 November to 12 December 2012, when geomorphic change at the McDonald Bridge gauging site was most pronounced because of sediment released from the former Lake Mills (East et al., 2015), the uncertainty of the reported discharge data was estimated to be 15%. The relative decrease in the rate of geomorphic change at the gauge from 12 December 2012 to 11 June 2013 warranted a decrease in the estimated uncertainty to 10%. Progressive geomorphic stabilization at the gauge location and modest flow conditions from June to September 2013 resulted in further reduction in estimated uncertainty to 8%.

Discharge was not reported at the Elwha River above Lake Mills water-quality gauge (USGS #12044900), but discharge values were estimated with discharge data from the McDonald Bridge gauge scaled using basin hydrology. Because a strong rainfall gradient affects the Elwha River catchment from south to north (Duda et al., 2011), the precipitation–volume ratio, that is, ratio of the product of precipitation depth and catchment area, was found to be a good predictor of discharge in the Elwha River main stem and its tributaries (Table 1). Precipitation depth and catchment area at river-point locations within the watershed were determined using USGS Streamstats (U.S. Geological Survey, 2014b). We found that discharge at Lake Mills was 82.5% of the discharge measured at the McDonald Bridge gauge. Uncertainty of these Lake Mills discharge estimates was assumed to be 20% greater than the estimated uncertainty at McDonald Bridge.

Stage, but not discharge, was measured in the lower Elwha River at the diversion weir (USGS gauge #12046260, Elwha River at Diversion) using a pressure transducer or acoustic Doppler velocimeter. To estimate discharge at the diversion weir, the discharge from the McDonald Bridge gauge was combined with gauged or estimated discharge from Little River and Indian Creek (the two largest tributaries entering the middle Elwha River) and an estimate from ungauged contributing areas. We also corrected for flood-wave routing between gauges. The Washington Department of Ecology gauged discharge on Little River (#18N050) from November 2002 until September 2012 and on Indian Creek (#18Q050) from May 2003 until September 2010 to an assumed uncertainty of 5%. To estimate discharge from Little River and Indian Creek during ungauged periods of the project, a modeled discharge ratio was constructed using overlapping data from 2006 to 2010 from the two tributaries relative to the McDonald Bridge gauge. The discharge ratio was found to be seasonal, changing by month, and averaged 3.9% for Little River and 4.3% for Indian Creek. Comparison of the predicted discharge using the discharge ratio for the two tributaries to the actual measured combined discharge from the Elwha River, Little River, and Indian Creek from 2006 to 2011 indicated that the discharge-ratio model predicted cumulative discharge to within 7% of the actual discharge 99% of the time. For this study, the uncertainty of predicted discharge from the tributaries using the ratio was assumed to be 15%. The discharge from 17 km^2 of ungauged catchment area at the diversion weir (Table 1) was calculated using the precipitation–volume ratio (Table 1), with an estimated uncertainty of 20%.

The diversion-weir gauge is 8 km downstream from the McDonald Bridge gauge. Analysis of flood peaks between gauges indicated the flood-wave travel time was about 6.7 h before the Elwha Dam removal (caused by flood-wave attenuation in Lake Aldwell) and 1.6 h after removal of Lake Aldwell (after May 2012). Empirical observations of flood-wave translation indicated that travel time between gauges decreased in a roughly piecewise linear fashion from September 2011 to April 2012. This piecewise linear progression of flood-wave translation was used to calculate the arrival time of given flow values from the McDonald Bridge gauge to the diversion-weir gauge, after correcting for inflows from tributaries.

Appendix B. Suspended-sediment sampling and sediment-surrogate methods

Physical samples of suspended sediment using standard USGS sampling protocol (Edwards and Glysson, 1999) were collected over a range of discharge and sediment-concentration conditions using cross-sectional and automated point sampling approaches. A total of 24 cross section sets of samples were collected from a pedestrian bridge located 350 m downstream from the diversion-weir gauge using a variety of depth-integrating, isokinetic samplers (D-61, D-74, and D-96; Davis, 2005). Sampling was opportunistic, requiring real-time monitoring of river conditions favorable for high concentrations (e.g., increased discharge and turbidity) and the rapid mobilization of field crews to sample a range of flow conditions, including high-discharge flows. Samples were processed to remove organic material leaving only the inorganic proportion of the suspended sediment, consistent with standard protocol, and loss-on-ignition data were recorded on select samples starting October 2012. Observations of the flowing river, river-channel deposits, and beach deposits at the Strait of Juan de Fuca showed perceptible fractions of particulate organic matter >2 mm, including large wood (Warrick et al., in this volume). However, no attempt was made to sample or quantify this load of particulate organic matter.

To increase the number of physical samples as well as provide a measure of redundancy in data collection, an automated point sampler (ISCO, Teledyne, Lincoln, NE) was operated at the diversion-weir gauge during the second year of the project. Subsample volumes of 200 mL were pumped every 6 h and composited into a single 800-mL daily sample for a total of 243 days from 10 September 2012 to 15 September 2013. The sampler intake was positioned to receive well-mixed water at the edge of the channel thalweg at a fixed point approximately 1.5 m above the channel bed and was housed in a plastic pipe fastened to the upstream-facing corner of a concrete abutment. To account for bias in SSC associated with the location of point samples, a cross-sectional coefficient of 1.92 was determined from the SSC correlation between concurrent cross section and point samples ($n = 10$) and each point sample SSC adjusted (Edwards and Glysson, 1999). Most sediment samples were analyzed for SSC and the percentage of silt and clay (particle size < 0.063 mm) at the USGS sediment laboratory at the Cascades Volcano Observatory in Vancouver, WA. Two samples, as well as all bedload samples, were analyzed at the USGS-certified GMA Hydrology sediment laboratory in Placerville, CA.

Two types of in situ turbidimeters, a DTS-12 nephelometer (Forest Technology Systems Ltd., 2012) and an Analite 180 optical-backscatter turbidity meter (McVan Instruments, 2000), were deployed at the diversion-weir gauge. Both turbidimeters use a monochrome, near-infrared light source with color compensation but differ in the angle of the detector relative to the angle of the incident light beam (Anderson, 2005). Nephelometers report measurements in formazin nephelometric units (FNU) and are best used in low-to-moderate

turbidity conditions (0–1000 FNU, e.g., most natural fluvial environments), whereas optical-backscatter meters report measurements in formazin backscatter units (FBU) and can measure in higher turbidity conditions (10–10,000 FBU) (Anderson, 2005). Both turbidimeters were mounted vertically on a concrete abutment at the diversion weir and enclosed in separate protective pipes designed for easy sensor retrieval and maintenance. Although the nephelometer manufacturer reports a maximum sensor range of 1600 FNU (Forest Technology Systems Ltd., 2012), we found evidence of sensor saturation for turbidity >1200 FNU and thus did not use values >1200 FNU in computing sediment loads. Turbidity data collected at 15-minute increments were telemetered to the USGS National Water Information System, and we calculated 15-minute SSC data for the study period (Curran et al., 2014).

Standard USGS guidelines were followed for maintaining in situ turbidimeters (Wagner et al., 2006) and for developing regression models for turbidity–SSC relations (Rasmussen et al., 2009). Transformation bias of SSC estimates was corrected using the approach of Duan (1983). Regressions were developed for both turbidimeters for total SSC as well as the concentration of silt and clay (<0.063 mm), the difference of which represents the sand component of SSC. The regression model for the nephelometer used a cube-root transformation for the SSC data (Curran et al., 2014). The regression model for the optical-backscatter turbidimeter used a standard logarithmic transformation for both turbidity and SSC.

From 13 November 2012 to 23 May 2013 the optical-backscatter instrument at the diversion-weir gauge malfunctioned. To augment these missing optical-backscatter data, a period of time when large sediment loads rendered nephelometric turbidity data unusable, available turbidity data from an optical-backscatter turbidimeter of the same manufacturer deployed at the McDonald Bridge gauge were used. Paired manual measurements of turbidity using a hand-held turbidimeter at the diversion-weir and McDonald Bridge gauges from 6 November 2012 to 28 December 2012, when the predominant sediment source was Lake Mills, indicated good correlation ($R^2 = 0.96$) of turbidity values between both gauges.

A 1500-kHz side-looking acoustic Doppler velocity meter (ADVM) Argonaut-SL was mounted proximal to turbidimeters on three separate deployments (1500-a, from 15 September 2011 to 4 December 2012; 1500-b, from 11 December 2012 to 11 January 2013; and 1500-c, from 23 January 2013 to 10 July 2013). Depending on the deployment, the ADVM were configured to measure 7–10 m lengths across the channel and perpendicular to flow, and cell sizes ranged from 0.7 to 2 m with the number of cells ranging from 5 to 10. Different ADVM configurations were needed to optimize data collection in changing channel conditions.

Multiple steps are required to post process raw acoustic backscatter data prior to developing relations with SSC, including correcting for instrument noise, beam spreading, fluid absorption, and calculating acoustic attenuation from absorption by sediments (Topping et al., 2004, 2006; Wood and Teasdale, 2013). Post-processing in this manner provided sediment-corrected backscatter (SCB) and a sediment attenuation coefficient, α_s, which were then used as explanatory variables in regression models developed to predict SSC (Wood and Teasdale, 2013). For this method, SSC and particle-size distribution (PSD) were assumed constant along the acoustic axis of the beam. Because instrument noise is unique for each instrument, separate regression models were developed for each ADVM deployment. The continuous 15-minute hydroacoustic data and concurrent SSC from cross section and auto-sampler point samples collected from 10 August 2011 through 10 July 2013 were used to develop different regression models and associated bias correction factors (Duan, 1983) for three separate deployments.

For the three 1500-kHz deployments (1500-a, -b, and -c), 281 SSC-surrogate pairs were used to develop regression models. The sediment attenuation coefficient (α_s) ranged from 0.1 to 15.7 dB/m for all models. In addition, a mean sediment corrected backscatter was needed to

develop the model for the first deployment (1500-a) and ranged from 79.3 to 114 dB.

Model performance was assessed on the basis of root-mean-square deviation (RMSD) normalized by the observed mean SSC and expressed as a percentage (Fig. B1). The RMSD was smallest for the nephelometer-SSC model (34%), and RMSD values for the optical-backscatter turbidimeter and hydroacoustic-SSC models were similar (46% and 47%,
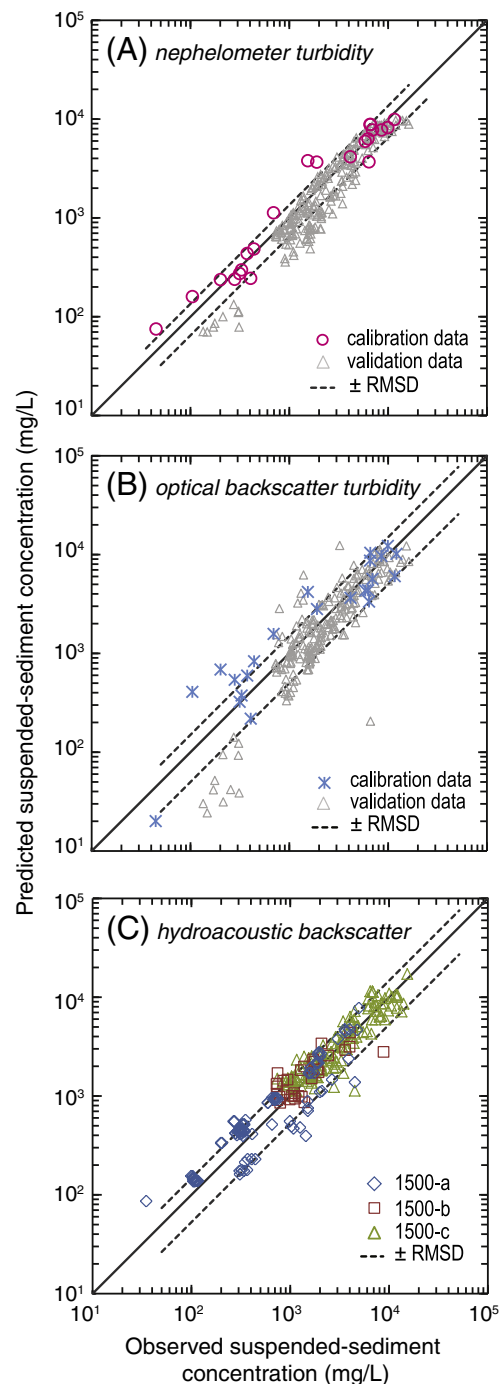

Fig. B1. Relations of predicted suspended-sediment concentration as a function of observed suspended-sediment concentration for each sediment-surrogate instrument: (A) nephelometer turbidity sensor, (B) optical-backscatter turbidity sensor, and (C) hydroacoustic Doppler 1500-MHz instrument. Cross-sectional suspended-sediment samples were used to construct the turbidity relations, while the cross-sectional suspended-sediment samples and the automated point samples were used to construct the hydroacoustic relation. Root mean square deviation (RMSD; one standard deviation of the prediction intervals) is shown for each relation.

respectively). For all models, the calibration data consisted of concurrent cross section samples and recorded sensor measurements. For models developed from hydroacoustic data, the calibration data set also consisted of SSC from automated point samples, which were needed to supplement the regression data set. The composite-averaged SSC value of all three sediment-surrogate instruments was also assessed against measured SSC with an RMSD of 47%. We assumed the composite-averaged reported SSC daily values had an uncertainty of 50%.

Appendix C. Supplementary data

Supplementary data associated with this article can be found in the online version, http://dx.doi.org/10.1016/j.geomorph.2014.12.032. These data include Google map of the most important areas described in this article.

References

Ahearn, D.S., Dahlgren, R.A., 2005. Sediment and nutrient dynamics following a low-head dam removal at Murphy Creek, California. Limnol. Oceanogr. 50 (6), 1752–1762.

American Rivers, 2014. 2013 Dam Removals. Website accessed on 14 May 2014 at. http://www.americanrivers.org/initiative/dams/projects/2013-dam-removals/.

American Rivers, Friends of the Earth, Trout Unlimited, 1999. Dam Removal Success Stories: Restoring Rivers Through Selective Removal of Dams That Don't Make Sense. 0-913890-96-0 (114 pp.).

Anderson, C.W., 2005. Field measurements: U.S. Geological Survey techniques of water-resources investigations. Book 9, Chapter A6, Section 6.7, Turbidity (version 2.1). U.S. Geological Survey National Field Manual for the Collection of Water-Quality Data (TWRI Book 9) (64 pp.).

Bänziger, R., Burch, H., 1990. Acoustic sensors (hydrophones) as indicators for bed load transport in a mountain torrent. Hydrology in Mountain Regions, Hydrological Measurements; the Water Cycle. Proceedings of two Lausanne Symposia, August. IAHS Publ. 193.

Bountry, J.A., Lai, Y.G., Randle, T.J., 2013. Sediment impacts from the Savage Rapids Dam removal, Rogue River, Oregon. In: De Graff, J.V., Evans, J.E. (Eds.), The Challenges of Dam Removal and River Restoration. Geological Society of America Reviews in Engineering Geology 21, pp. 93–104. http://dx.doi.org/10.1130/2013.4121(08).

Brenkman, S.J., Pess, G.R., Torgersen, C.E., Kloehn, K.K., Duda, J.J., Corbett, S.C., 2008. Predicting recolonization patterns and interactions between potamodromous and anadromous salmonids in response to dam removal in the Elwha River, Washington State, USA. Northwest. Sci. 82 (Special Issue), 91–106.

Brenkman, S.J., Duda, J.J., Torgersen, C.E., Welty, E., Pess, G.R., Peters, R., McHenery, M.L., 2012. A riverscape perspective of Pacific salmonids and aquatic habitats prior to large-scale dam removal in the Elwha River, Washington, USA. Fish. Manag. Ecol. 19, 36–53.

Brune, G.M., 1953. Trap efficiency of reservoirs. Trans. Am. Geophys. Union 34, 407–418.

Cannatelli, K., Curran, J., 2012. Importance of hydrology on channel evolution following dam removal: case study and conceptual model. J. Hydraul. Eng. 138 (5), 377–390. http://dx.doi.org/10.1061/(ASCE)HY.1943-7900.0000526.

Childers, D., 1999. Field comparisons of six pressure-difference bedload samplers in high-energy flow. U.S. Geological Survey Water Resources Investigations Report 92-4068 (59 pp.).

Childers, D., Kresch, D.L., Gustafson, S.A., Randle, T.J., Melena, T., Cluer, B., 2000. Hydrologic data collected during the 1994 Lake Mills drawdown experiment, Elwha River, Washington. U.S. Geological Survey Water-Resources Investigations Report 99-4215 (115 pp.).

Church, M., Krishnappan, B.G., 1998. Sediment sources, transport processes, and modeling approaches for the Fraser River. In: Gray, C., Tuominen, T. (Eds.), Health of the Fraser River Aquatic Ecosystem: Environment Canada, DOE FRAP 1998-11 (18 pp.).

Cohn, T.A., 2005. Estimating contaminant loads in rivers: an application of adjusted maximum likelihood to type 1 censored data. Water Resour. Res. 41 (7), W07003. http://dx.doi.org/10.1029/2004wr003833.

Crane, J., 2011. Finding the River: An Environmental History of the Elwha. Oregon State University Press, Corvallis (256 pp.).

Curran, C.A., Konrad, C.P., Higgins, J.L., Bryant, M.K., 2009. Estimates of sediment load prior to dam removal in the Elwha River, Clallam County, Washington. U.S. Geological Survey Scientific Investigations Report 2009-5221 (18 pp.).

Curran, C.A., Magirl, C.S., Duda, J.J., 2014. Suspended-sediment concentrations during dam decommissioning in the Elwha River, Washington. U.S. Geological Survey Data Set http://dx.doi.org/10.5066/F7M043DB (http://wa.water.usgs.gov/pubs/misc/elwha/ssc/).

Czuba, C.R., Randle, T.J., Bountry, J.A., Magirl, C.S., Czuba, J.A., Curran, C.A., Konrad, C.P., 2011a. Anticipated sediment delivery to the lower Elwha River estuary during and following dam removal. In: Duda, J.J., Warrick, J.A., Magirl, C.S. (Eds.), Coastal Habitats of the Elwha River, Washington—Biological and Physical Patterns and Processes Prior to Dam Removal: U.S. Geological Survey Scientific Investigations Report 2011-5120, pp. 27–46.

Czuba, J.A., Magirl, C.S., Czuba, C.R., Grossman, E.E., Curran, C.A., Gendaszek, A.S., Dinicola, R.S., 2011b. Sediment load from major rivers into Puget Sound and its adjacent waters. U.S. Geological Survey Fact Sheetpp. 2011–3083.

Czuba, J.A., Magirl, C.S., Czuba, C.R., Curran, C.A., Johnson, K.H., Olsen, T.D., Kimball, H.K., Gish, C.C., 2012. Geomorphic analysis of the river response to sedimentation downstream of Mount Rainier, Washington. U.S. Geological Survey Open-File Report 2012-1242 (134 pp.).

Davis, B.E., 2005. A guide to the proper selection and use of federally approved sediment and water-quality samplers. U.S. Geological Survey Open-File Report 2005-1087 (20 pp.).

Doyle, M.W., Stanley, E.M., Harbor, J.M., 2002. Geomorphic analogies for assessing probable channel response to dam removal. J. Am. Water Resour. Assoc. 38 (6), 1567–1579. http://dx.doi.org/10.1111/j.1752-1688.2002.tb04365.x.

Doyle, M.W., Harbor, J.M., Stanley, E.H., 2003a. Toward policies and decision-making for dam removal. Environ. Manag. 31, 453–465. http://dx.doi.org/10.1007/s00267-002-2819-z.

Doyle, M.W., Stanley, E.H., Harbor, J.M., 2003b. Channel adjustments following two dam removals in Wisconsin. Water Resour. Res. 39 (1:1011). http://dx.doi.org/10.1029/2002WR001714.

Duan, N., 1983. Smearing estimate: a nonparametric retransformation method. J. Am. Stat. Assoc. 78 (383), 605–610.

Duda, J.J., Freilich, J.E., Schreiner, E.G., 2008. Baseline studies in the Elwha River ecosystem prior to dam removal. Northwest. Sci. 82 (Special Issue), 1–12. http://dx.doi.org/10.3955/0029-344X-82.S.I.1.

Duda, J.J., Warrick, J.A., Magirl, C.S., 2011. Coastal and lower Elwha River, Washington, prior to dam removal—History, status, and defining characteristics. In: Duda, J.J., Warrick, J.A., Magirl, C.S. (Eds.), Coastal Habitats of the Elwha River, Washington—Biological and Physical Patterns and Processes Prior to Dam Removal: U.S. Geological Survey Scientific Investigations Report 2011-5120, pp. 1–26.

East, A.E., Pess, G.R., Bountry, J.A., Magirl, C.S., Ritchie, A.C., Logan, J.B., Randle, T.J., Mastin, M.C., Minear, J.T., Duda, J.J., Liermann, M.C., McHenry, M.L., Beechie, T.J., Shafroth, P.B., 2015. Large-scale dam removal on the Elwha River, Washington, USA: river channel and floodplain geomorphic change. Geomorphology 228, 765–786. http://dx.doi.org/10.1016/j.geomorph.2014.08.028.

Edwards, T.K., Glysson, G.D., 1999. Field methods for measurement of fluvial sediment. U.S. Geological Survey Techniques of Water-Resources Investigations, Book 3, Chapter C2.

Einstein, H.A., 1937. The bed load transport as probability problem. Mitteilung der Versuchsanstalt fuer Wasserbau an der Eidgenössischen Technischen Hochschule, Zurich (110 pp.).

Erdman Video Services, 2013. Elwha River Restoration Project webcams: Erdman Video Systems, Inc., in collaboration with the National Park Service. Website, accessed 18 December 2013, at. http://video-monitoring.com/construction/olympic/js.htm.

Forest Technology Systems, Ltd., 2012. DTS-12 SDI Turbidity Sensor: FTS User Manual, rev. 15 (January 13, 2012, 24 pp.).

Gelfenbaum, G., Duda, J.J., Warrick, J.A., 2011. Summary and anticipated responses to Elwha River dam removal. In: Duda, J.J., Warrick, J.A., Magirl, C.S. (Eds.), Coastal Habitats of the Elwha River, Washington—Biological and Physical Patterns and Processes Prior to Dam Removal: U.S. Geological Survey Scientific Investigations Report 2011-5120, pp. 249–263.

Gelfenbaum, G., Stevens, A.W., Miller, A., Warrick, J.A., Ogston, A.S., Eidam, E., 2015. Large-scale dam removal on the Elwha River, Washington, USA: coastal geomorphic change. Geomorphology. http://dx.doi.org/10.1016/j.geomorph.2015.01.002 (in this volume).

Gomez, B., Troutman, B.M., 1997. Evaluation of process errors in bed load sampling using a dune model. Water Resour. Res. 33, 2387–2398.

Gomez, B., Hubble, D.W., Stevens, H.H., 1990. At-a-point bed load sampling in the presence of dunes. Water Resour. Res. 26, 2717–2731.

Gowan, C., Stephenson, K., Shabman, L., 2006. The role of ecosystem valuation in environmental decision making: hydropower relicensing and dam removal on the Elwha River. Ecol. Econ. 56 (4), 508–523.

Graf, W.L., 1999. Dam nation: a geographic census of American dams and their large-scale hydrologic impacts. Water Resour. 35, 1305–1311.

Guy, H.P., 1970. Fluvial sediment concepts. U.S. Geological Survey Techniques of Water-Resource Investigation 03-C1, Book 3 — Chapter C1 (55 pp.).

Habersack, H.M., 2001. Radio-tracking gravel particles in a large braided river in New Zealand: a field test of the stochastic theory of bed load transport proposed by Einstein. Hydrol. Process. 15, 377–391.

Hammond, S.E., 1989. Comparison of sediment transport formulas and computation of sediment discharges for the North Fork Toutle and Toutle rivers, near Mount St. Helens, Washington. U.S. Geological Survey Open-File Report 88-463 (18 pp.).

Heinz Center, 2002. Dam Removal: Science and Decision Making. The H. John Heinz III Center for Science, Economics and the Environment, Washington D.C. (221 pp.).

Heinz Center, 2003. Dam Removal Research: Status and Prospects. In: Graf, W.L. (Ed.), The H. John Heinz III Center for Science, Economics and the Environment, Washington D.C. (151 pp.).

Hilldale, R.C., Carpenter, W.O., Goodwiller, B., Chambers, J.P., Randle, T.J., 2014. Installation and preliminary calibration of impact plates to continuously measure bed load: Elwha River, WA, USA. J. Hydraul. Eng. http://dx.doi.org/10.1061/(ASCE)HY.1943-7900.0000975.

Hubbell, D.W., Stevens, H.H., 1986. Factors affecting accuracy of bedload sampling. Proceedings of the Fourth Federal Interagency Sedimentation Conference March 24–27, 1986, Las Vegas, Nevada. v. 1.

Johnson, P.R.S., 2013. Elwha: Value of a River, Managing Risk in the Pacific Northwest. (Ph.D. Thesis). Yale University, New Haven, Connecticut.

Johnson, T.E., Pizzuto, J., Egan, J., Bushaw-Newton, K.L., Hart, D.D., Lawrence, J., Lynch, E., 2001. The Manatawny Creek Dam removal: project overview and geomorphic characteristics. Bull. N. Am. Benthol. Soc. 18, 121–122.

Kammerer, J.C., 1990. Largest rivers in the United States. U.S. Geological Survey Fact Sheet 87-242.

Kloehn, K.K., Beechie, T.J., Morley, S.A., Coe, H.J., Duda, J.J., 2008. Influence of dams on river-floodplain dynamics in the Elwha River, Washington. Northwest. Sci. 82 (Special Issue), 224–235.

Konrad, C.P., 2009. Simulating the recovery of suspended sediment transport and river-bed stability in response to dam removal on the Elwha River, Washington. Ecol. Eng. 35 (7), 1104–1115. http://dx.doi.org/10.1016/j.ecoleng.2009.03.018.

Lipman, P.W., Mullineaux, D.R., 1981. The 1980 eruptions of Mount St. Helens, Washington. U.S. Geological Survey Professional Paper 1250 (844 pp.).

Madej, M.A., Ozaki, V., 1996. Channel response to sediment wave propagation and movement, Redwood Creek, California, USA. Earth Surf. Process. Landf. 21, 911–927.

Magirl, C.S., Connolly, P.J., Coffin, B., Duda, J.J., Curran, C.A., Draut, A.E., 2010. Sediment management strategies associated with dam removal in the State of Washington. Paper Presented at Proceedings of the 2nd Joint Federal Interagency Conference, Las Vegas, NV, 28 June–July 1.

Major, J.J., 2004. Posteruption suspended sediment transport at Mount St. Helens: decadal-scale relationships with landscape adjustments and river discharges. J. Geophys. Res. 109, F01002. http://dx.doi.org/10.1029/2002JF000010.

Major, J.J., O'Connor, J.E., Podolak, C.J., Keith, M.K., Grant, G.E., Spicer, K.R., Pittman, S., Bragg, H.M., Wallick, J.R., Tanner, D.Q., Rhode, A., Wilcock, P.R., 2012. Geomorphic response of the Sandy River, Oregon, to removal of Marmot Dam. U.S. Geological Survey Professional Paper 1792 (64 pp.).

McVan Instruments Pty Ltd, 2000. NEP 180 and 190 Series Instructions: The ANALITE 180, 190 and 195 Turbidity Probe (10/00, V9, 8 pp.).

Meade, R.H., Parker, R.S., 1985. Sediment in rivers of the United States. National Water Summary 1984, Hydrologic Events, Selected Water-Quality Trends, and Ground-Water Resources by U.S. Geological Survey. U.S. Geological Survey Water-Supply Paper 2275, pp. 49–60.

Naik, P.K., Jay, D.A., 2011. Distinguishing human and climate influences on the Columbia River: changes in mean flow and sediment transport. J. Hydrol. 404 (3–4), 259–277. http://dx.doi.org/10.1016/j.jhydrol.2011.04.035.

Neiman, P.J., Schick, L.J., Ralph, F.M., Hughes, M., Wick, G.A., 2011. Flooding in western Washington: the connection to atmospheric rivers. J. Hydrometeorol. 12, 1337–1358. http://dx.doi.org/10.1175/2011JHM1358.1.

Nolan, K.M., Kelsey, H.M., Marron, D.C., 1995. Geomorphic processes and aquatic habitat in the Redwood Creek basin, northwestern California. U.S. Geological Survey Professional Paper 1454 (304 pp.).

NRCS (National Resources Conservation Service), 2014. SNOTEL Update Report. Website, accessed 10 April 2014, at. http://www.wcc.nrcs.usda.gov/reports/SelectUpdateReport.html.

O'Connor, J., Major, J., Grant, G., 2008. The dams come down—unchaining U.S. rivers. Geotimes 53 (3), 22–28.

Pearson, A.J., Snyder, N.P., Collins, M.J., 2011. Rates and processes of channel response to dam removal with a sand-filled impoundment. Water Resour. Res. 47, W08504. http://dx.doi.org/10.1029/2010wr009733.

Pess, G.R., McHenry, M.L., Beechie, T.J., Davies, J., 2008. Biological impacts of the Elwha River dams and potential salmonid responses to dam removal. Northwest. Sci. 82 (Special Issue), 72–90.

Pizzuto, J., 2002. Effects of dam removal on river form and process. Bioscience 52 (8), 683–691. http://dx.doi.org/10.1641/0006-3568(2002)052[0683:EODROR]2.0.CO;2.

Poff, N.L., Hart, D.D., 2002. How dams vary and why it matters for the emerging science of dam removal. Bioscience 52 (8), 659–668. http://dx.doi.org/10.1641/0006-3568(2002)052[0659:HDVAWI]2.0.CO;2.

Randle, T.J., Young, C.A., Melena, J.T., Ouellette, E.M., 1996. Sediment analysis and modeling of the river erosion alternative. U.S. Bureau of Reclamation, Pacific Northwest Region, Elwha Technical Series PN-95-9 (138 pp.).

Randle, T.J., Bountry, J.A., Ritchie, A., Wille, K., 2015. Large-scale dam removal on the Elwha River, Washington, USA: erosion of reservoir sediment. Geomorphology (in this volume).

Rantz, S.E., 1982. Measurement and computation of streamflow: volume 2, computation of discharge. U.S. Geological Survey Water-Supply Paper 2175pp. 285–631.

Rasmussen, P.P., Gray, J.R., Glysson, G.D., Ziegler, A.C., 2009. Guidelines and procedures for computing time-series suspended-sediment concentrations and loads from in-stream turbidity-sensor and streamflow data. U.S. Geological Survey Techniques and Methods, Book 3, Chap. C4 (53 pp.).

Rickenmann, D., McArdell, B.W., 2007. Continuous measurement of sediment transport in the Erlenback stream using piezoelectric bedload sensors. Earth Surf. Process. Landf. 32, 1362–1378. http://dx.doi.org/10.1002/esp.1478.

Rickenmann, D., McArdell, B.W., 2008. Calibration of piezoelectric bedload sensors in the Pitzbach mountain stream. Geodin. Acta 21/1-2, 35–52. http://dx.doi.org/10.3166/ga21.35-52.

Rickenmann, D., Turowski, J.M., Fritschi, B., Wyss, C., Laronne, J., Barzilai, R., Reid, I., Kreisler, A., Aigner, J., Seitz, H., Habersack, H., 2014. Bedload transport measurements with impact plate geophones: comparison of sensor calibration in different gravel-bed streams. Earth Surf. Process. Landf. 39, 928–942. http://dx.doi.org/10.1002/esp.3499.

Riggsbee, J.A., Julian, J.P., Doyle, M.W., Wetzel, R.G., 2007. Suspended sediment, dissolved organic carbon, and dissolved nitrogen export during the dam removal process. Water Resour. Res. 43, W09414. http://dx.doi.org/10.1029/2006wr005318.

Runkel, R.L., Crawford, C.G., Cohn, T.A., 2004. Load estimator (LOADEST): a FORTRAN program for estimating constituent loads in streams and rivers. U.S. Geological Survey Techniques and Methods Book 4, Chapter A5 (69 pp.).

Sando, S.K., Lambing, J.H., 2011. Estimated loads of suspended sediment and selected trace elements transported through the Clark Fork Basin, Montana, in selected periods before and after the breach of Milltown Dam (water years 1985–2009). U.S. Geological Survey Scientific Investigations Report 2011-5030 (64 pp.).

Taylor, J.R., 1997. An Introduction to Error Analysis. University Science Books, Sausalito, Calif (327 pp.).

Topping, D.J., Melis, T.S., Rubin, D.M., Wright, S.A., 2004. High-resolution monitoring of suspended-sediment concentration and grain size in the Colorado River in Grand Canyon using a laser acoustic system. Proceedings of the 9th International Symposium on River Sedimentation, Yichang, China, 18–21 October. Tsinghua University Press, pp. 2507–2514.

Topping, D.J., Wright, S.A., Melis, T.S., Rubin, D.M., 2006. High-resolution monitoring of suspended-sediment concentration and grain size in the Colorado River using laser-diffraction instruments and a three-frequency acoustic system. Proceedings of the 8th Federal Inter-Agency Sedimentation Conference, Reno, NV, 2–6 April 2006, pp. 555–559.

U.S. Army Corps of Engineers, 2013. National Inventory of Dams. U.S. Army Corps of Engineers (web site, website accessed 23 April 2014, at https://geo.usace.army.mil/pgis/f?p=397:1:10488455857785).

U.S. Department of the Interior, National Park Service, 1995. Elwha River Ecosystem Restoration, Final Environmental Impact Statement. NPS D-253A, Olympic National Park, WA.

U.S. Department of the Interior, National Park Service, 1996. Elwha River Ecosystem Restoration Implementation, Final Environmental Impact Statement. NPS D-271A, Olympic National Park, Port Angeles, WA.

U.S. Department of the Interior, Department of Commerce, Lower Elwha S'Klallam Tribe, 1994. The Elwha report—restoration of the Elwha River ecosystem and native anadromous fisheries. A Report to Congress Submitted Pursuant to Public Law 102-495, Port Angeles, WA.

U.S. Geological Survey, 2014a. The StreamStats Program for Washington. Website, accessed 10 March 2014, at. http://water.usgs.gov/osw/streamstats/Washington.html.

U.S. Geological Survey, 2014b. National Water Information System, U.S. Geological Survey Database. Website, accessed February 21, 2014, at. http://waterdata.usgs.gov/wa/nwis/nwis.

Wagner, R.J., Boulger Jr., R.W., Oblinger, C.J., Smith, B.A., 2006. Guidelines and standard procedures for continuous water-quality monitors: Station operation, record computation, and data reporting. U.S. Geological Survey Techniques and Methods 1-D3 (51 pp.).

Ward, L., Crain, P., Freymond, B., McHenry, M., Morrill, D., Pess, G., Peters, R., Shaffer, J., Winter, B., Wunderlich, B., 2008. Elwha River Fish Restoration Plan—developed pursuant to the Elwha River Fisheries Restoration Act, Public Law 102-495. U.S. Department of Commerce, National Oceanic and Atmospheric Administration NMFS-NWFSC-90, Seattle, WA (169 pp.).

Warrick, J.A., Draut, A.E., McHenery, M.L., Miller, I.M., Magirl, C.S., Beirne, M.M., Stevens, A.W., Logan, J.B., 2011. Geomorphology of the Elwha River and its delta. In: Duda, J.J., Warrick, J.A., Magirl, C.S. (Eds.), Coastal Habitats of the Elwha River, Washington—Biological and Physical Patterns and Processes Prior to Dam Removal: U.S. Geological Survey Scientific Investigations Report 2011-5120, pp. 47–73.

Warrick, J.A., Duda, J.J., Magirl, C.S., Curran, C.A., 2012. River turbidity and sediment loads during dam removal. Eos 93, 425–426. http://dx.doi.org/10.1029/2012EO430002.

Warrick, J.A., Madej, M.A., Goñi, M.A., Wheatcroft, R.A., 2013. Trends in the suspended-sediment yields of coastal rivers of northern California, 1955–2010. J. Hydrol. 489, 108–123. http://dx.doi.org/10.1016/j.jhydrol.2013.02.041.

Warrick, J.A., Bountry, J.A., East, A.E., Magirl, C.M., Randle, T.J., Gelfenbaum, G., Pess, G.R., Duda, J.J., 2015. Large-scale dam removal on the Elwha River, Washington, USA: source-to-sink sediment budget and synthesis. Geomorphology (in this volume).

Whitelaw, E., MacMullan, E., 2002. A framework for estimating the costs and benefits of dam removal. Bioscience 52 (8), 724–730. http://dx.doi.org/10.1641/0006-3568(2002)052[0724:AFFETC]2.0.CO;2.

Wilcox, A.C., O'Connor, J.E., Major, J.J., 2014. Rapid reservoir erosion, hyperconcentrated flow, and downstream deposition triggered by breaching of 38-m-tall Condit Dam, White Salmon River, Washington. J. Geophys. Res. Earth Surf. http://dx.doi.org/10.1002/2013jf003073 (2013JF003073).

Wildman, L.A.S., MacBroom, J.G., 2005. The evolution of gravel bed channels after dam removal: case study of the Anaconda and Union City Dam removals. Geomorphology 71 (1–2), 245–262. http://dx.doi.org/10.1016/j.geomorph.2004.08.018.

Winter, B.D., Crain, P., 2008. Making the case for ecosystem restoration by dam removal in the Elwha River, Washington. Northwest. Sci. 82 (Special Issue), 13–28.

Wood, M.S., Teasdale, G.N., 2013. Use of surrogate technologies to estimate suspended sediment in the Clearwater River, Idaho, and Snake River, Washington, 2008-10. U.S. Geological Survey Scientific Investigations Report 2013-5052 (30 pp.).

Wunderlich, R.C., Winter, B.D., Meyer, J.H., 1994. Restoration of the Elwha River ecosystem. Fisheries 19, 11–19.